Space-based interferometer to IMAGE the surface of habitable planets around Sun-like stars

Project 3, Astronomical Optics, Spring 2013

Introduction

Craig McNabb

Goals

Space-based interferometer to IMAGE the surface of habitable planets around Sun-like stars

- Imaging nearby exoplanet surfaces with a space-based interferometer
- Use space-based network of large telescopes to image nearby exoplanet surfaces
- Each telescope will have high precision AO system + coronagraph to cancel starlight
- Planet image obtained by coherent combination of telescope beams
- How many telescopes ?
- How large ?
- Baseline ?
- # of targets
- Spectroscopy ?

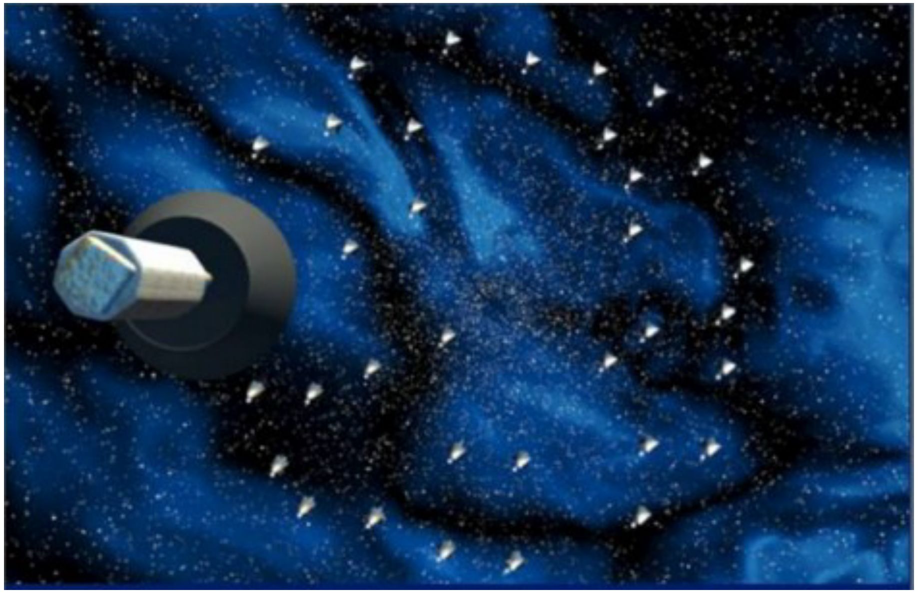

Overview of the Project

- Identified scientific goals for imaging Earth-like exoplanets
  - Goals are for "nearby" exoplanets both confirmed and anticipated
  - Imaging provides the ability to distinguish areas on the planet
    - Includes rocky areas, water, vegetation, etc.
- Developed a concept system capable of meeting (most of) the scientific goals
- Developed a simple exoplanet interferometry budget tool
  - Uses inputs from the team to calculate the predicted performance of the interferometer array
- Mechanical and Optical designs were explored and will be presented

The Team

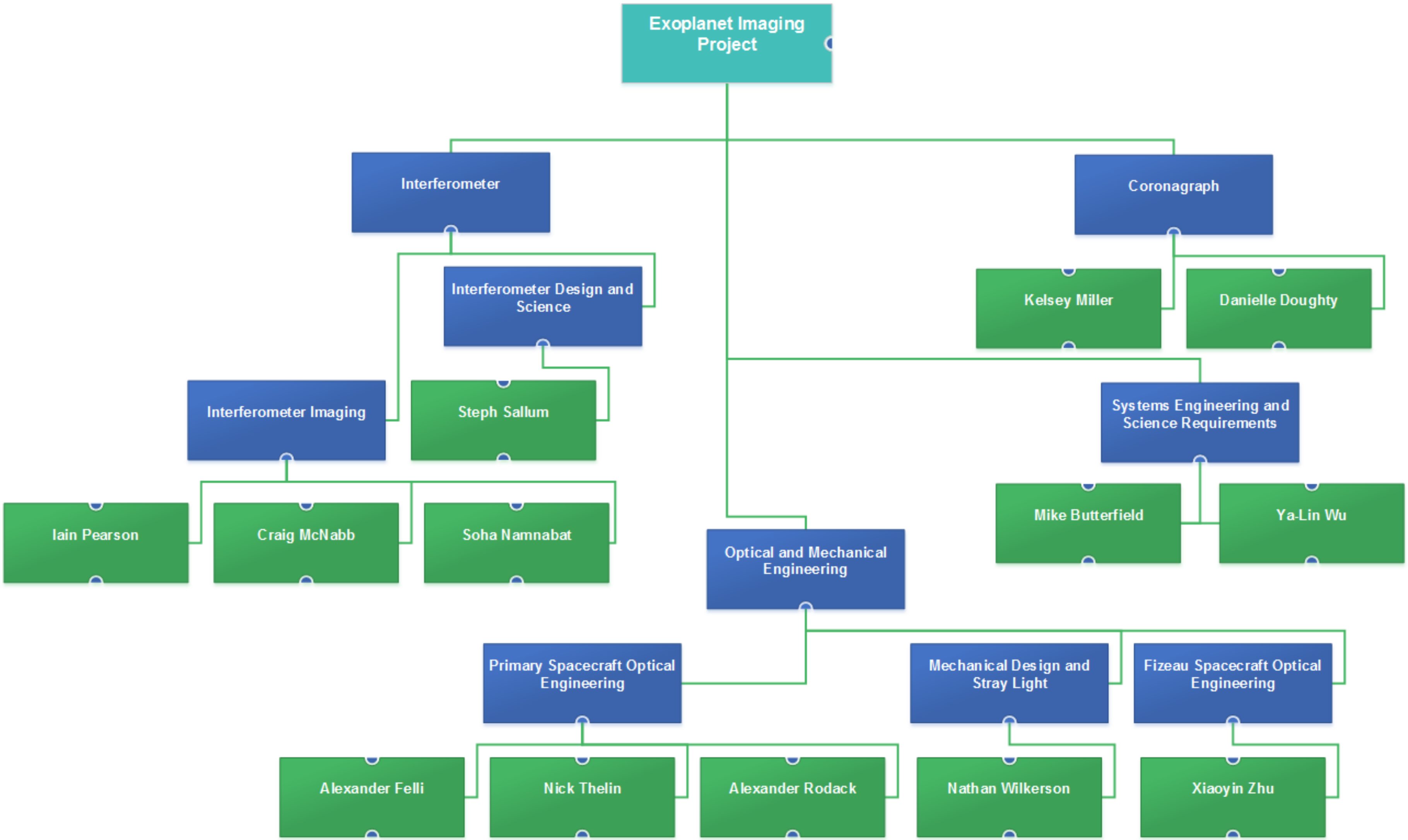
Exoplanet Imaging Project
Interferometer
Coronagraph
Interferometer Design and Science
Kelsey Miller
Danielle Doughty
Interferometer Imaging
Steph Sallum
Systems Engineering and Science Requirements
Iain Pearson
Craig McNabb
Soha Namnabat
Mike Butterfield
Ya-Lin Wu
Optical and Mechanical Engineering
Primary Spacecraft Optical Engineering
Mechanical Design and Stray Light
Fizeau Spacecraft Optical Engineering
Alexander Felli
Nick Thelin
Alexander Rodack
Nathan Wilkerson
Xiaoyin Zhu

Science

Mike Butterfield
Ya-Lin Wu
Steph Sallum

Science Goals

IMAGE the surface of habitable planets around Sun-like stars

- Imaging nearby exoplanet surfaces with a space-based interferometer
- Use space-based network of large telescopes to image nearby exoplanet surfaces
- Each telescope will have high precision AO system + coronagraph to cancel starlight
- Planet image obtained by coherent combination of telescope beams
- How many telescopes ?
- How large ?
- Baseline ?
- # of targets
- Spectroscopy ?

Quick rundown of relevant quantities

Distances from Earth:

- Distance from Milky Way to Andromeda Galaxy: 2.5 Mly
- Milky Way Diameter: 100 - 120 kly (~10^21 m)
  - Distance to center of Milky Way: 27.2 kly (~10^17 m)
  - ~80 kly to most distant star in Milky Way
- Nearest star: Proxima Centauri: 4.2 ly
  - 19000 times closer than the farthest Milky Way star
- Nearest identified Exoplanet Alpha Centauri Bb: 4.23 ly
- Nearest high ESI Exoplanet Gliese 581 g: 20.2 ly
  - Very high ESI (announced last week): 1033.8 ly
    - 18 times closer than the farthest Milky Way star

Ranges of star and terrestrial exoplanet parameters:

- Quick note: no real consensus exists on what defines "terrestrial"
  - Not gas giants
  - Within the solar system terrestrial means Mercury, Venus, Earth, and Mars
- Terrestrial or "rocky" exoplanets
  - Radius ~0.5 to ~3 times Earth's radius
  - Mass ~0.01 to ~100 times Earth's mass
  - Semi-major Axis: ~0.01 to ~1.5 AU
  - Estimated 40% of stars have orbiting exoplanets

What and how many out there?

- ~50 stars within 15 ly; 4 have planets

  Alpha Cen B (1 earth-sized planet; "lava world")

  Gliese 674 (1 hot Neptune)

  Epsilon Eridani (1 hot Jupiter)

  Tau Ceti (5 earth-sized planets?)

- We have a few targets; maybe more in future

  icecap

  continent

  marine

  signs of civilizations...

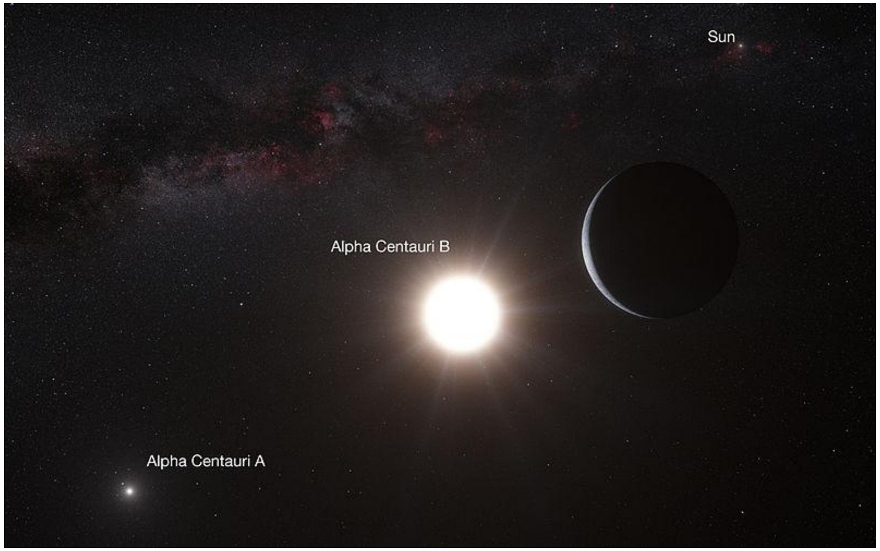

TPF Top 10 Target Stars (wikipedia)

Rank [6]	Target star	Constellation	Distance (light-years)	Spectral type
1	Alpha Centauri A	Centaurus	4.3	G2V
2	Alpha Centauri B	Centaurus	4.3	K1V
3	Tau Ceti	Cetus	12	G8V
4	Eta Cassiopeiae	Cassiopeia	19	G3V
5	Beta Hydri	Hydrus	24	G2IV
6	Delta Pavonis	Pavo	20	G8V
7	Pi3 Orionis	Orion	26	F6V
8	Gamma Leporis	Lepus	29	F7V
9	Epsilon Eridani	Eridanus	10	K2V
10	40 Eridani	Eridanus	16	K1V

Nearest Terrestrial Exoplanets (Wiki)

Table

Name	Image (artist concept)	Mass ($M_⊕$)	Radius ($R_⊕$)	Surface gravity (g)	Surface temperature	Semi-major axis (AU)	Eccen-tricity	Earth Similarity Index	Habitability	Main source	Distance from the Sun (ly)
Alpha Centauri Bb	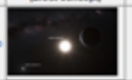	≥1.1			1200 K	0.04			Orbits too close to the star		4.23
Tau Ceti e		≥4.3	≥1.6		343 K	0.552 ± 0.02	0.05±0.02	0.77	Thermoplanet Orbits on inner edge of habitable zone		11.90
Tau Ceti f		≥6.6			233–323 K	1.35 ± 0.1	0.03 ± 0.3	0.71	Psychroplanet Orbits on outer edge of habitable zone		11.90
Gliese 876 d[1]		6.8			157–377°C[2] (estimate)	0.021	0.21		Too hot	[3]	15
82 G. Eridani b		≥2.7				0.1207	0		Orbits too close to the star	[4]	19.71
82 G. Eridani c		≥2.4				0.2036	0		Orbits too close to the star	[4]	19.71
82 G. Eridani d		≥4.8			388 K[5]	0.3499	0		Orbits too close to the star	[4]	19.71
Gliese 581 e		≥1.7				0.029	0		It is unlikely to possess an atmosphere due to its high temperature	[6]	20
Gliese 581 c[7]		≥5.6				0.072	0		Questionable. Likely to lie outside the habitable zone[8]	[9]	20
Gliese 581 d[10]		≥5.6	2.34[11]	1.27[11]	233 K[11]	0.218	0	0.69[11]	Psychroplanet.[11] Lies within the habitable zone[12]	[13]	20
Gliese 667C b		6.30		1.44	445 K	0.05	0.09		Too hot	[11]	22
Gliese 667C c[14][15]		6.24		1.32	302 K	0.13	0.34	0.82	Mesoplanet	[11]	22
61 Virginis b[16]		≥5.1				0.050	0.12		Orbits too close to the star	[17]	28
HD 85512 b[18]	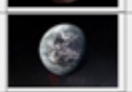	≥3.6	1.74[11]	1.33[11]	361 K[11]	0.26	0.11	0.76[11]	Thermoplanet.[11] Was considered to be the best candidate for habitability[19] until discovery of Gliese 667C c.	[19]	36
55 Cancri e		8.6				0.016	0.17		Orbits too close to the star	[20]	40
HD 40307 b[21]		≥4.2				0.047	0.2		Orbits too close to the star	[22]	42
HD 40307 c[21]		≥6.8				0.081	0.06		Orbits too close to the star	[22]	42
HD 40307 d[23]	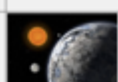	≥9.2				0.134	0.07		Orbits too close to the star	[24]	42
HD 40307 e		≥3.5				0.1886	0.15		Orbits too close to the star	[25]	42
HD 40307 f		≥5.2				0.247	0.02		Orbits too close to the star	[25]	42
HD 40307 g		≥7.1			279 K[26]	0.600	0.29	0.79[27]	Mesoplanet	[25]	42

In September 2012, the discovery of two planets orbiting Gliese 163[28] was announced.[29][30] One of the planets, Gliese 163 c, about 6.9 times the mass of Earth and somewhat hotter, was considered to be within the habitable zone, but is probably not terrestrial.[29][30]

Earth-like planet appearance in the mid-IR

What information do we want to obtain?

- Surface (or near surface) temperature
  - 300K peak is ~10 microns
  - Identification of water boiling and freezing points would be useful
  - Resolved temperature at poles and equator would be useful
    - Requires ~3 to 10 linear imaging elements across the planet depending on ultimate goal
- Spectral emissions
  - H20, CH4, O3, CO2, etc.
  - Spectral range of 1 to 50 microns would be excellent
    - Spectral resolution of ~1 micron would be sufficient to see bulk features of H20 and C02
- If H20, CH4, and O3 are found simultaneously, it is very strong evidence of the presence of life.

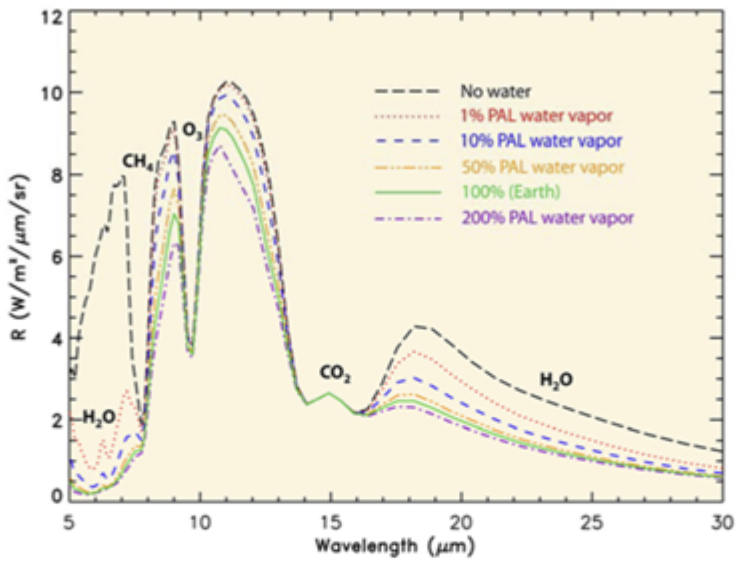

http://exep.jpl.nasa.gov/files/exep/tpfl414.pdf

Exo-Zodiacal Light Background

- The exozodiacal dust IR emissions are the primary contribution to the interferometer's background signal
  - For a quick estimate, a column the width of the telescope's diffraction limited spot size at the exoplanet-earth range of 4.7 light years was defined
  - The blackbody emissions over the interferometer's spectral range were calculated and the radiometric contribution was found to be 3-4 orders of magnitude smaller than that of the from the exoplanet
  - Assumptions include a EZ particle density of 1e-16 particles/m^3, a 6 to 10 meter telescope
    - Uses a simplified particle temperature model - could be improved
- The calculated exozodiacal background contribution was incorporated into the system design spreadsheet

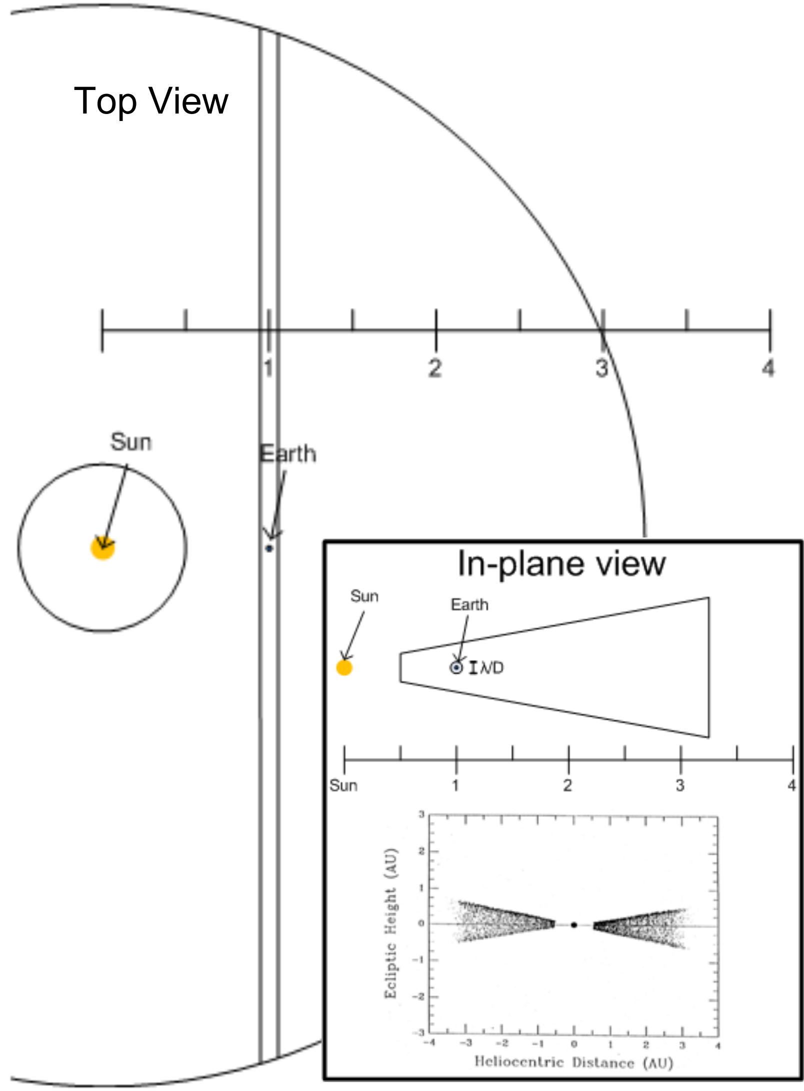

Exoplanet Imaging Geometry and Variables

Important geometric factors include:

- Angular separation of the planet-star system
- Diameter of the exoplanet
- Distance from the interferometer to the planet (semi-major axis)

Important variables include

- Background contributions
- Star temperature
- Exozodiacal dust density

These factors drive:

- Subaperture diameter
- Interferometer baseline
- Spectral detection range
- (Effectively all aspects of the interferometer)

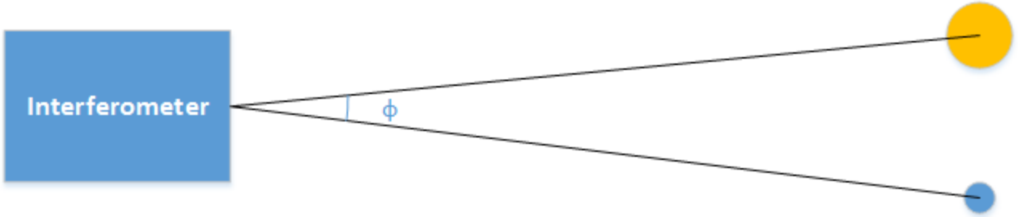

What can infrared emissivity tell us?

IEEE GEOSCIENCE AND REMOTE SENSING LETTERS, VOL. 4, NO. 1, JANUARY 2007

Evidence of Low Land Surface Thermal Infrared Emissivity in the Presence of Dry Vegetation

Albert Olioso, Guillem Sòria, José Sobrino, and Benoit Duchemin

TABLE I
LAND SURFACE EMISSIVITY AND NDVI MEASURED NEAR MARRAKECH, MOROCCO, ON MARCH 10–11, 2003. MEASUREMENT STANDARD DEVIATIONS ARE PRESENTED IN BRACKETS. VALUES FOR WHEAT AND WET BARLEY WERE OBTAINED FROM THE MEAN OF THE THREE LARGEST MEASURED VALUES (ALL OF THEM AT A LARGE CANOPY COVER). FOR DRY BARLEY, THE VALUE AT THE LARGEST NDVI IS GIVEN

	Emissivity				NDVI
	8-13 µm	11.5-12.5 µm	10.3-11.3 µm	8.2-9.2 µm	
Wheat at large NDVI	0.981 (+/- 0.006)	0.984 (+/- 0.006)	0.976 (+/- 0.009)	0.964 (+/- 0.016)	0.85 (+/- 0.004)
Wet Barley	0.981 (+/- 0.003)	0.981 (+/- 0.003)	0.972 (+/- 0.004)	0.958 (+/- 0.005)	0.85 (+/- 0.005)
Dry Barley	0.963 (+/- 0.006)	0.968 (+/- 0.005)	0.953 (+/- 0.005)	0.934 (+/- 0.007)	0.64 (+/- 0.006)
Soil in the wheat field	0.957 (+/- 0.002)	0.978 (+/- 0.001)	0.964 (+/- 0.002)	0.911 (+/- 0.004)	0.17 (+/- 0.003)
Soil in the barley field	0.958 (+/-0.004)	0.980 (+/-0.002)	0.965 (+/-0.003)	0.923 (+/- 0.002)	0.29 (+/- 0.013)

Spectral radiometer + IR lamp for BB calibration

Bottom line:

Soil < Dry Plants < Moist Plants

What can infrared emissivity tell us?

Spectral emissivity measurements of Mercury's surface indicate Mg- and Ca-rich mineralogy, K-spar, Na-rich plagioclase, rutile, with possible perovskite, and garnet

A.L. Sprague[a,*], K.L. Donaldson Hanna[b], R.W.H. Kozlowski[c], J. Helbert[d], A. Maturilli[d], J.B. Warell[e], J.L. Hora[f]

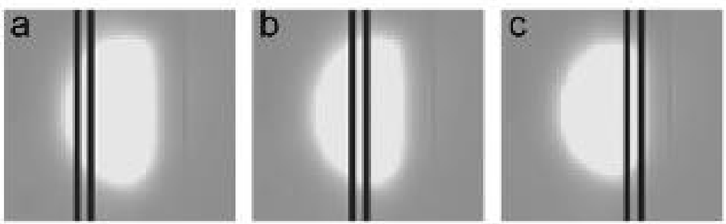

Fig. 3. Images, taken in MIRSI's imaging mode, just prior to the spectral image integration for (a) RBC, (b) DPWCB, and (c) CB. The location and width of the MIRSI spectrograph slit at the time of integration is indicated by the parallel black lines.

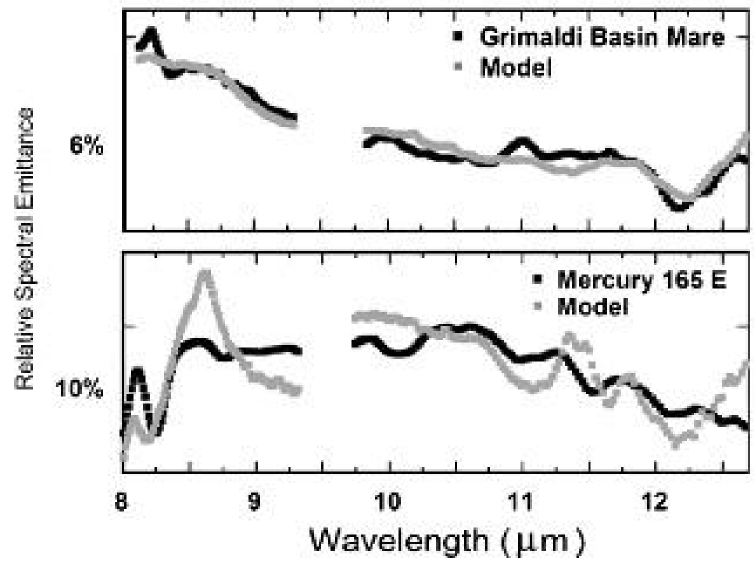

Fig. 6. Lunar (top) and Mercury (bottom) spectra are fit using the same set of minerals from the spectral library used to fit several lunar spectra (Donaldson Hanna et al., 2007). We were not able to achieve a good best fit with the lunar mineral spectral library. For discussion see Section 6, page 15.

Take spectra...

...compare to models or lab data.

System Design

Steph Sallum
Mike Butterfield

Block Diagram and Array Layout

The array is composed of two spacecraft types:

1. The primary array spacecraft (orange)
2. The Fizeau focus spacecraft (blue)

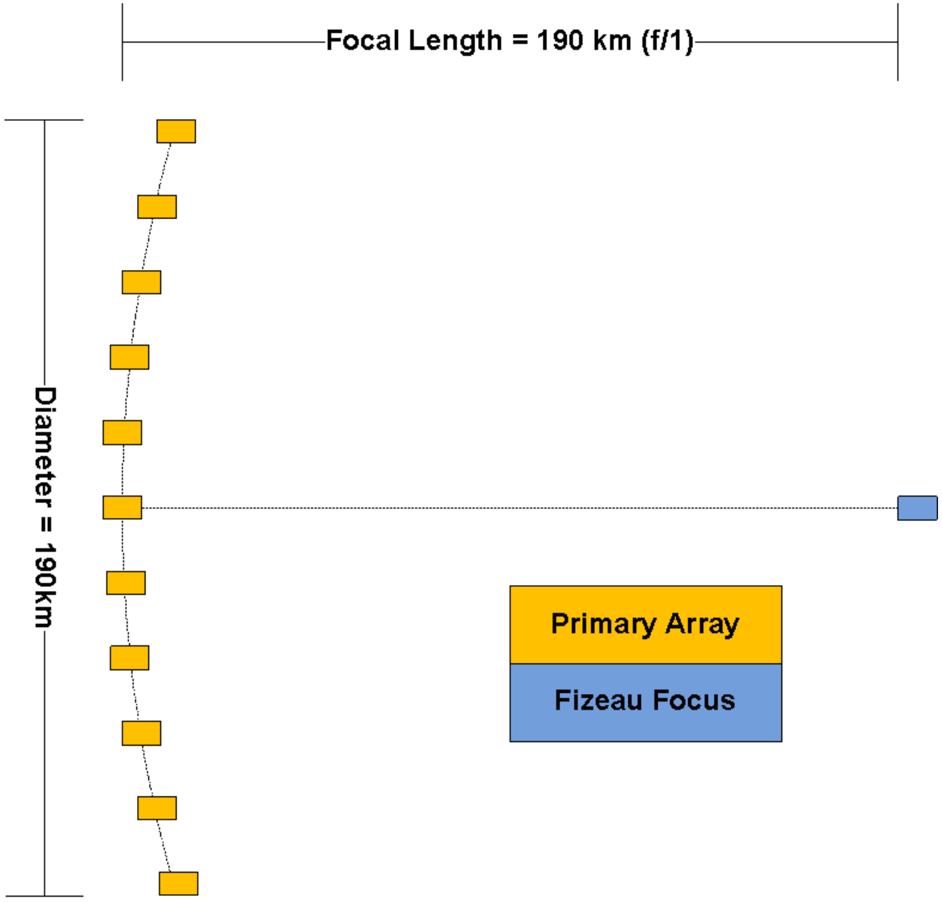

Primary Aperture Spacecraft Block Diagram

Basic optical path: Right to Left

Telescope, Beam splitter sends light down two paths

1. Short wavelengths (~1 to ~50 microns) Adaptive Optics / Coronagraph Path
   a. Star signal is removed from this path
2. Long wavelengths (~50 to ~100 microns)
   a. Star signal remains in this path to be used in the interferometer's "bootstrapping" process

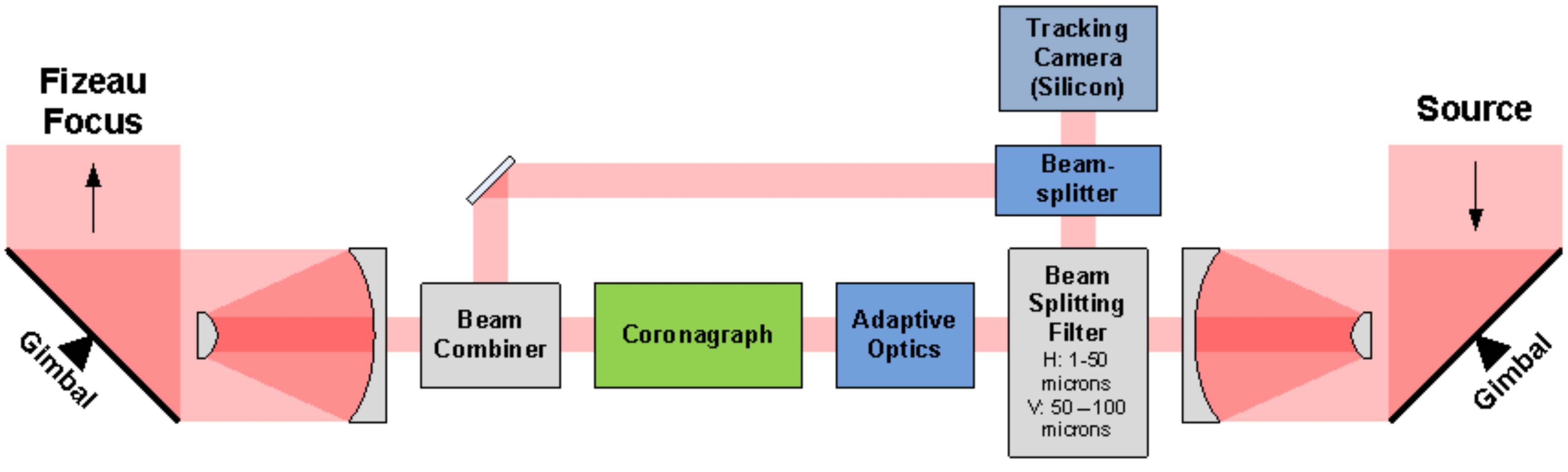

Imaging Instrument Spacecraft Optical Block Diagram

- The Imaging Instrument Spacecraft optical system is comprised of collecting optics, a tracking system, the pupil densification system, a beamsplitter and two imaging instruments
  - Shorter wavelengths are the science wavelengths used for measuring the planet
  - Longer wavelengths still contain light from the star and are used for bootstrapping the interferometer
- Not shown in this block diagram is the control system, data processing, and other systems that would reside on this spacecraft

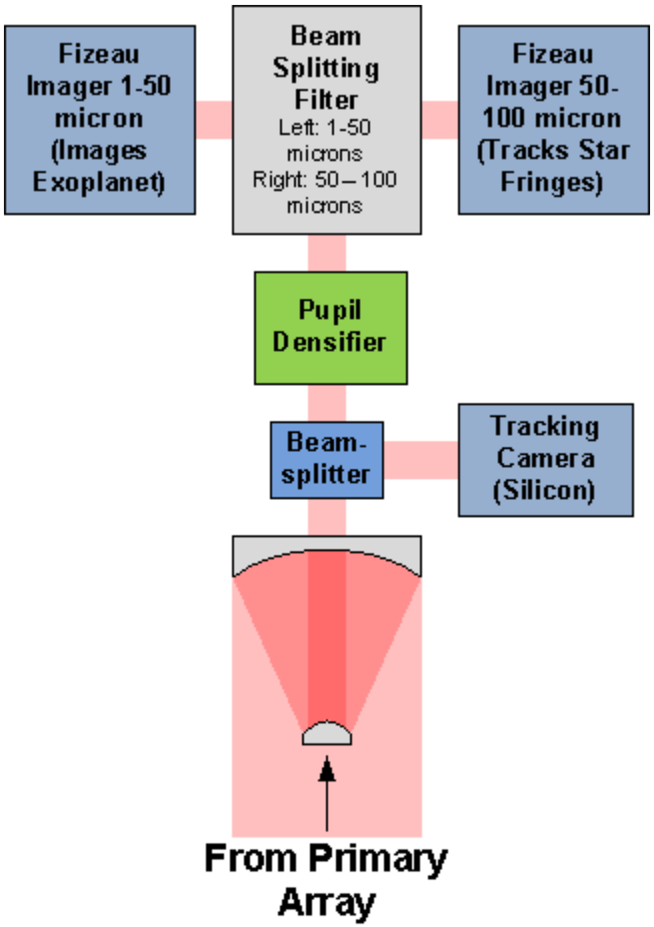

System SNR Budget Tool

- Used to determine the SNR based on the system's constraints
- Incorporates
  - Telescope parameters
  - Optical system throughput
    Exoplanet properties
    - Orbit, temperature, etc.
  - Exozodiacal dust estimates
  - Planck's law blackbody emission calculations
  - Science instrument spectral range
- Implements the simple exozodiacal dust background calculation presented in the science section

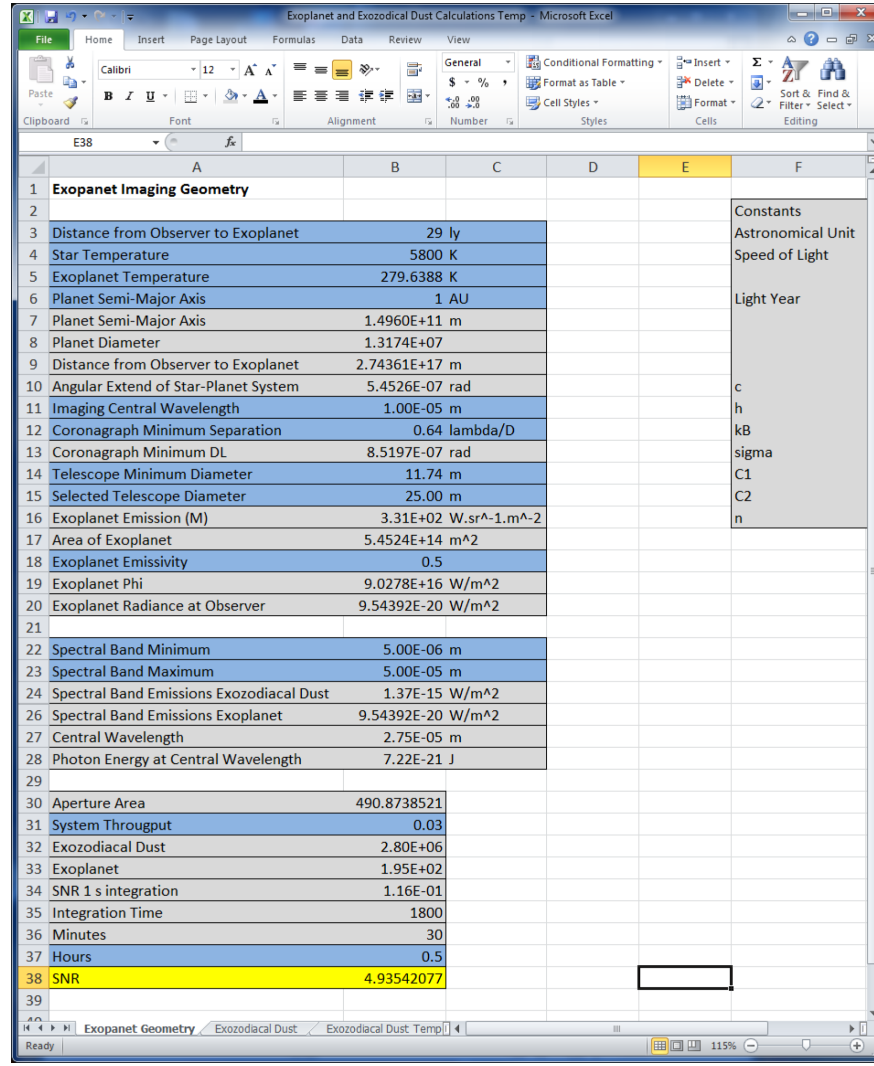

	A	B	C	D	E	F
1	**Exopanet Imaging Geometry**					
2						Constants
3	Distance from Observer to Exoplanet	29	ly			Astronomical Unit
4	Star Temperature	5800	K			Speed of Light
5	Exoplanet Temperature	279.6388	K			
6	Planet Semi-Major Axis	1	AU			Light Year
7	Planet Semi-Major Axis	1.4960E+11	m			
8	Planet Diameter	1.3174E+07				
9	Distance from Observer to Exoplanet	2.74361E+17	m			
10	Angular Extend of Star-Planet System	5.4526E-07	rad			c
11	Imaging Central Wavelength	1.00E-05	m			h
12	Coronagraph Minimum Separation	0.64	lambda/D			kB
13	Coronagraph Minimum DL	8.5197E-07	rad			sigma
14	Telescope Minimum Diameter	11.74	m			C1
15	Selected Telescope Diameter	25.00	m			C2
16	Exoplanet Emission (M)	3.31E+02	W.sr^-1.m^-2			n
17	Area of Exoplanet	5.4524E+14	m^2			
18	Exoplanet Emissivity	0.5				
19	Exoplanet Phi	9.0278E+16	W/m^2			
20	Exoplanet Radiance at Observer	9.54392E-20	W/m^2			
21						
22	Spectral Band Minimum	5.00E-06	m			
23	Spectral Band Maximum	5.00E-05	m			
24	Spectral Band Emissions Exozodiacal Dust	1.37E-15	W/m^2			
26	Spectral Band Emissions Exoplanet	9.54392E-20	W/m^2			
27	Central Wavelength	2.75E-05	m			
28	Photon Energy at Central Wavelength	7.22E-21	J			
29						
30	Aperture Area	490.8738521				
31	System Througput	0.03				
32	Exozodiacal Dust	2.80E+06				
33	Exoplanet	1.95E+02				
34	SNR 1 s integration	1.16E-01				
35	Integration Time	1800				
36	Minutes	30				
37	Hours	0.5				
38	SNR	4.93542077				
39						

Exoplanet Imaging Interferometer System Design Tool

Tool results:

- The photon noise limit at 10 lightyears says that a 3 m aperture with an integration time of 600 s will give an SNR of > 5
  - This does not include background contributions
- The exozodiacal dust signal is the largest contributor to the background
  - For an earth analog at 10 ly, a 4.05 m (coronagraph-driven minimum) aperture requires an integration time of 75 minutes
  - Increasing the aperture to 10 m reduces the integration time to 2 minutes
- For our TPF top 10 stars with good exoplanet potential, ~29 lightyears is the longest distance
  - This would require an 11.74m coronagraph-driven aperture diamter
    - Results in an 11 hour integration time
  - To get down to a few minute integration time, a really large aperture would be required (25 meters and 30 minutes integration time)

Detector Considerations

Beyond Fourth-generation IR detectors will drastically simplify the design of this system

- We did not perform an exhaustive design of this system and assume that a high spatial and spectral density IR detector will be available
- MKID was suggested by Olivier
  - Provides photon arrival time and energy
  - Available in a large array (> 1000x1000)
  - Very low noise - photon noise limited
- Advanced versions of the MKID array are an assumption of this design
  - However, the system SNR budget provides a 3dB (50%) loss for the spectroscopy instrument assuming some sort of spectrometer
  - No further design of the spectroscopy instrument has been performed
  - The next-gen-MKID "magical" array will hopefully provide a significant reduction in throughput losses

Interferometer Layout

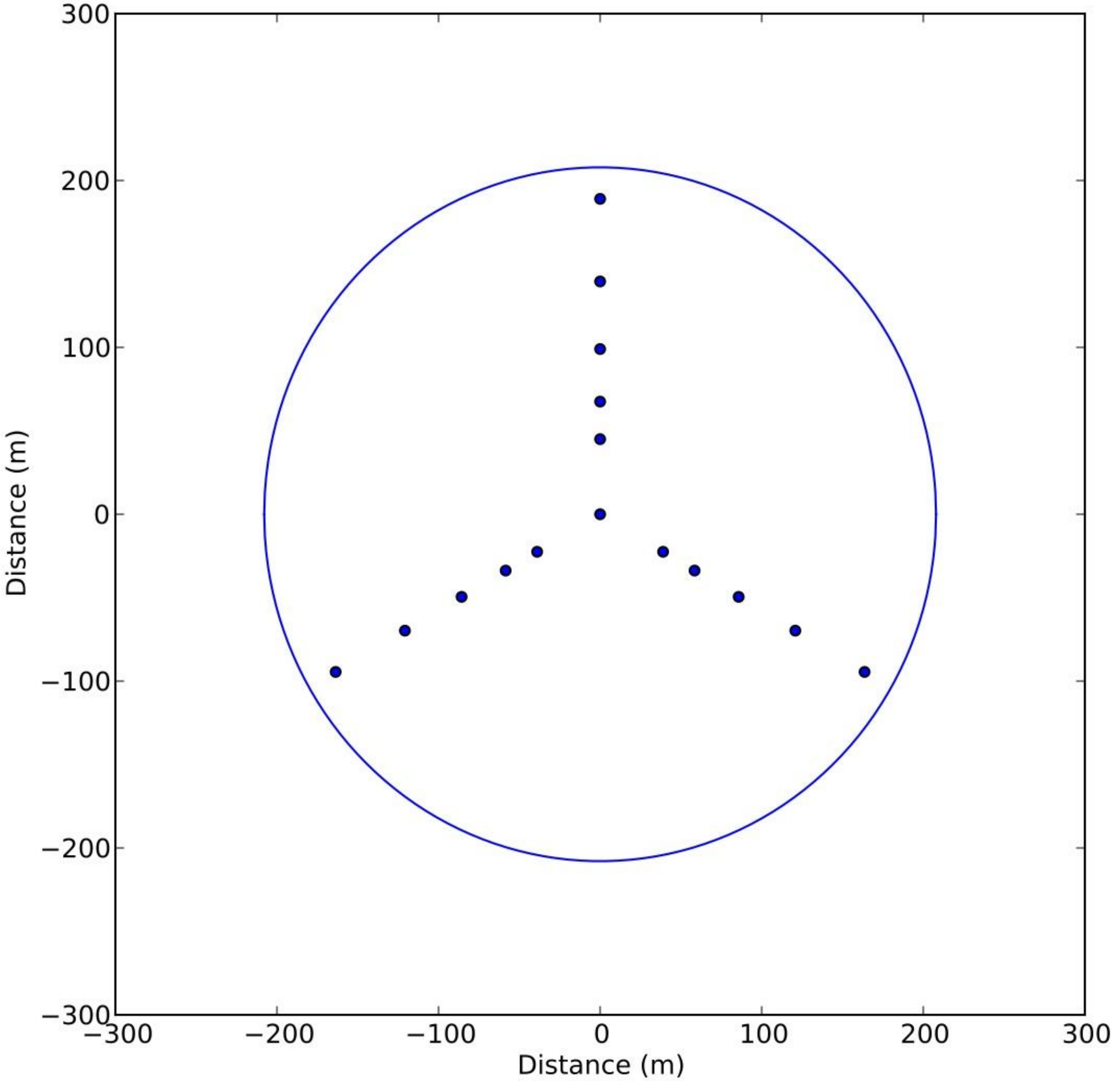

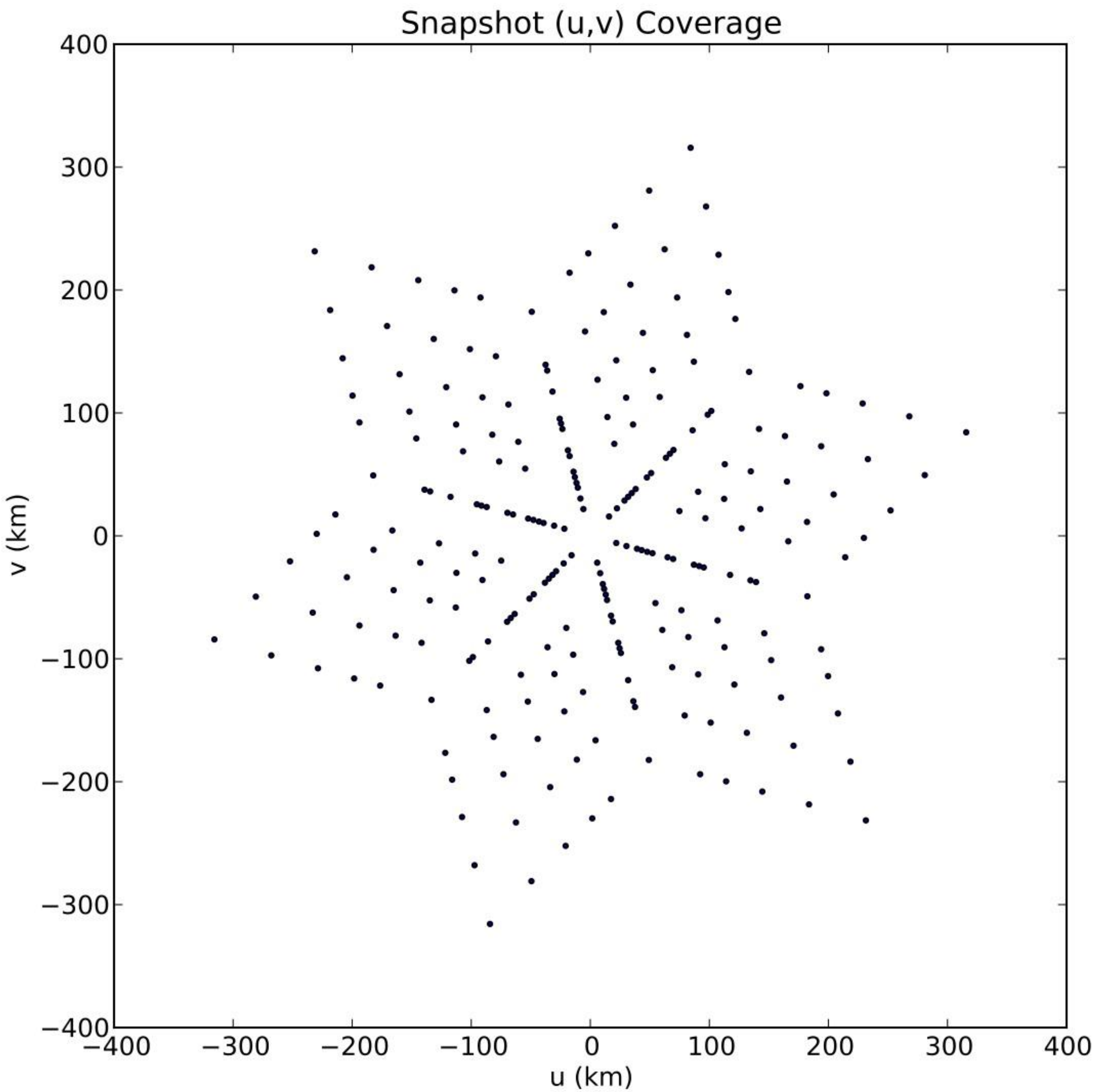

Snapshot (u,v) Coverage
400
300
200
100
0
−100
−200
−300
−400
v (km)
−400
−300
−200
−100
0
100
200
300
400
u (km)

Resolution

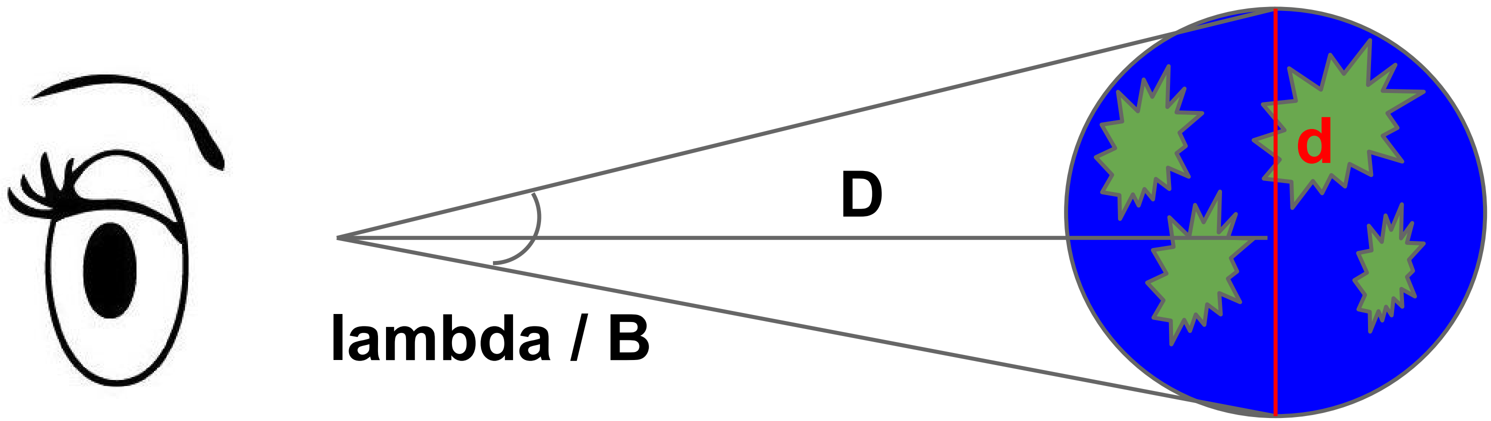

For each baseline length B, calculate the spatial scale corresponding to lambda/B at a distance D.

d ~ (lambda*D)/B

1 Earth diameter ~ 10 microns*20 light years / 150 km

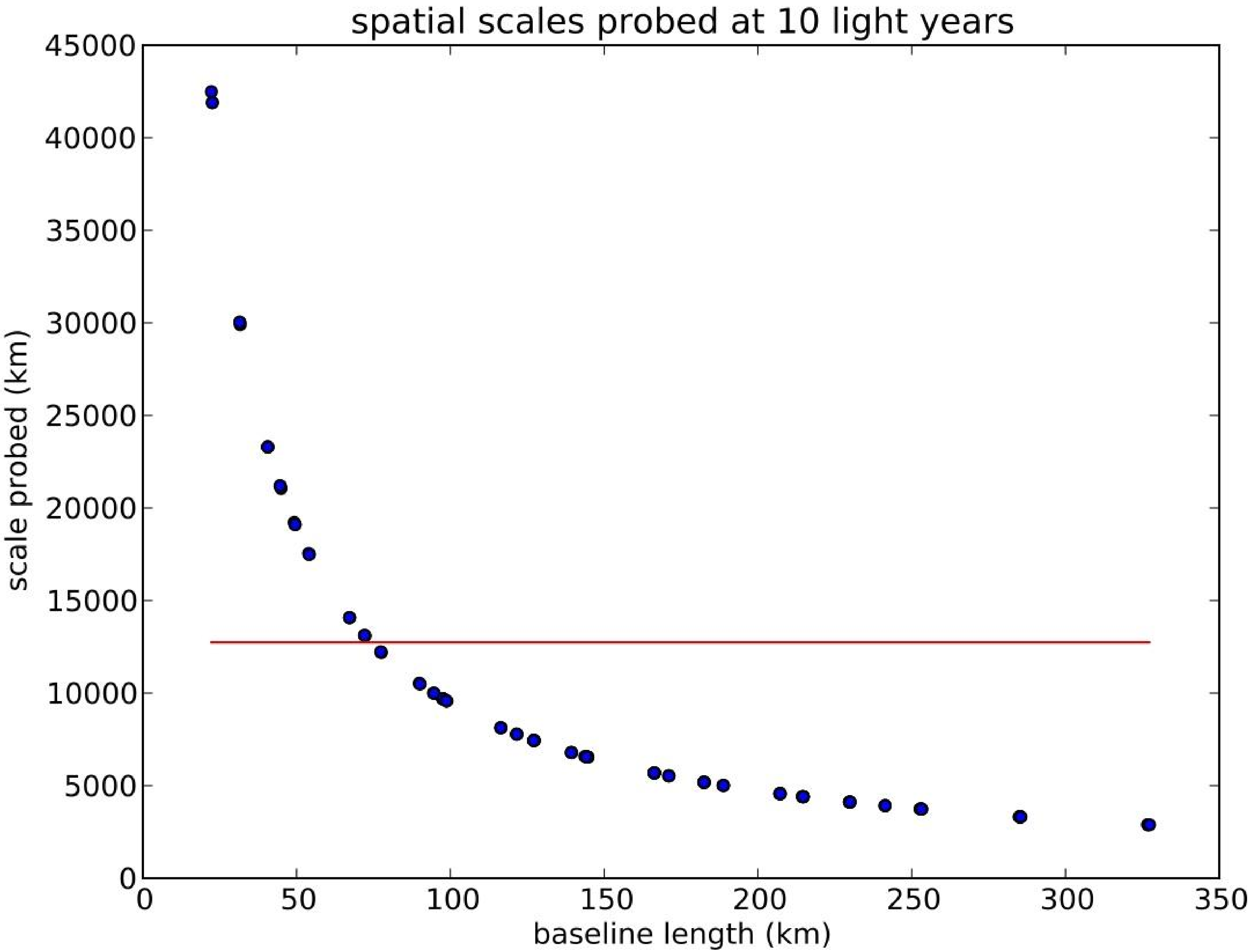

spatial scales probed at 10 light years
scale probed (km)
baseline length (km)
45000
40000
35000
30000
25000
20000
15000
10000
5000
0
0
50
100
150
200
250
300
350

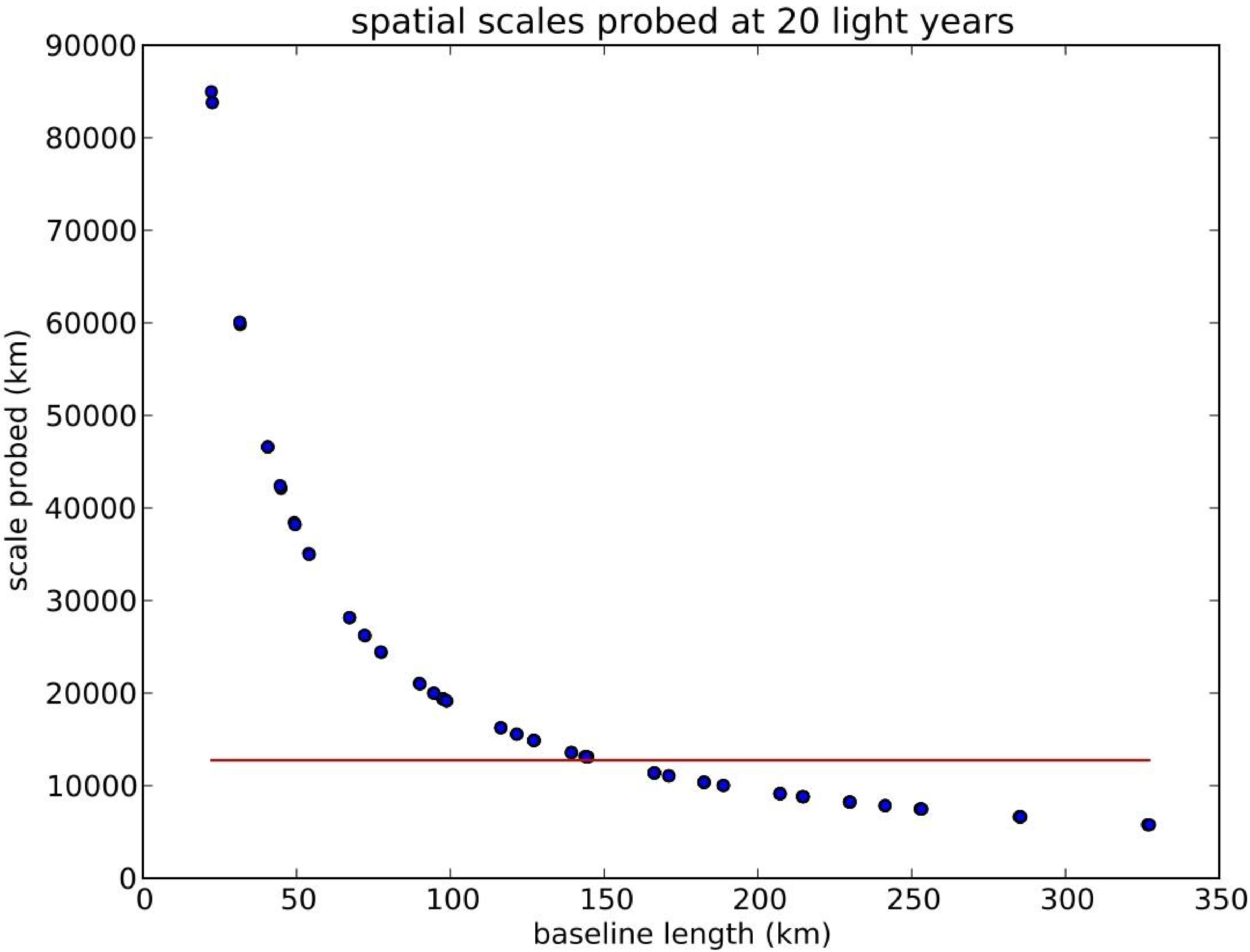
spatial scales probed at 20 light years
scale probed (km)
baseline length (km)
90000
80000
70000
60000
50000
40000
30000
20000
10000
0
0
50
100
150
200
250
300
350

Planet Detection Algorithms

Some important considerations:

- No residual noise due to atmospheric turbulence
- Extremely long distance from mirror array to detector
- Sky doesn’t rotate over the course of an observation

These factors will affect the performance of detection algorithms

ADI and LOCI

- Big problem in ground-based imaging is slowly-varying (or “quasistatic”) speckles
- Don’t rotate the telescope, let the sky rotate over the duration of the observation instead
- Quasistatic speckles are fixed with the pupil, therefore easier to subtract (LOCI)
- In our case we’ll still get quasistatic speckles but the sky won’t be rotating

Statistical Methods

- Ideal linear observer requires inverse of the full covariance matrix for the data
- Sources of noise:
  - Quasistatic fluctuations and residual phase errors from AO system
  - Noise in the science and wavefront sensor cameras
  - Randomness in the object being viewed

Statistical Methods

- Covariance matrix is very large
- We can decompose it into the sum of the *diagonal* covariance matrix for the science camera and the covariance for all other sources of randomness
- Use the Woodbury matrix inversion formula to make the inverse computationally feasible
- Algorithm does not require ADI data

Demonstration of Hotelling Observer

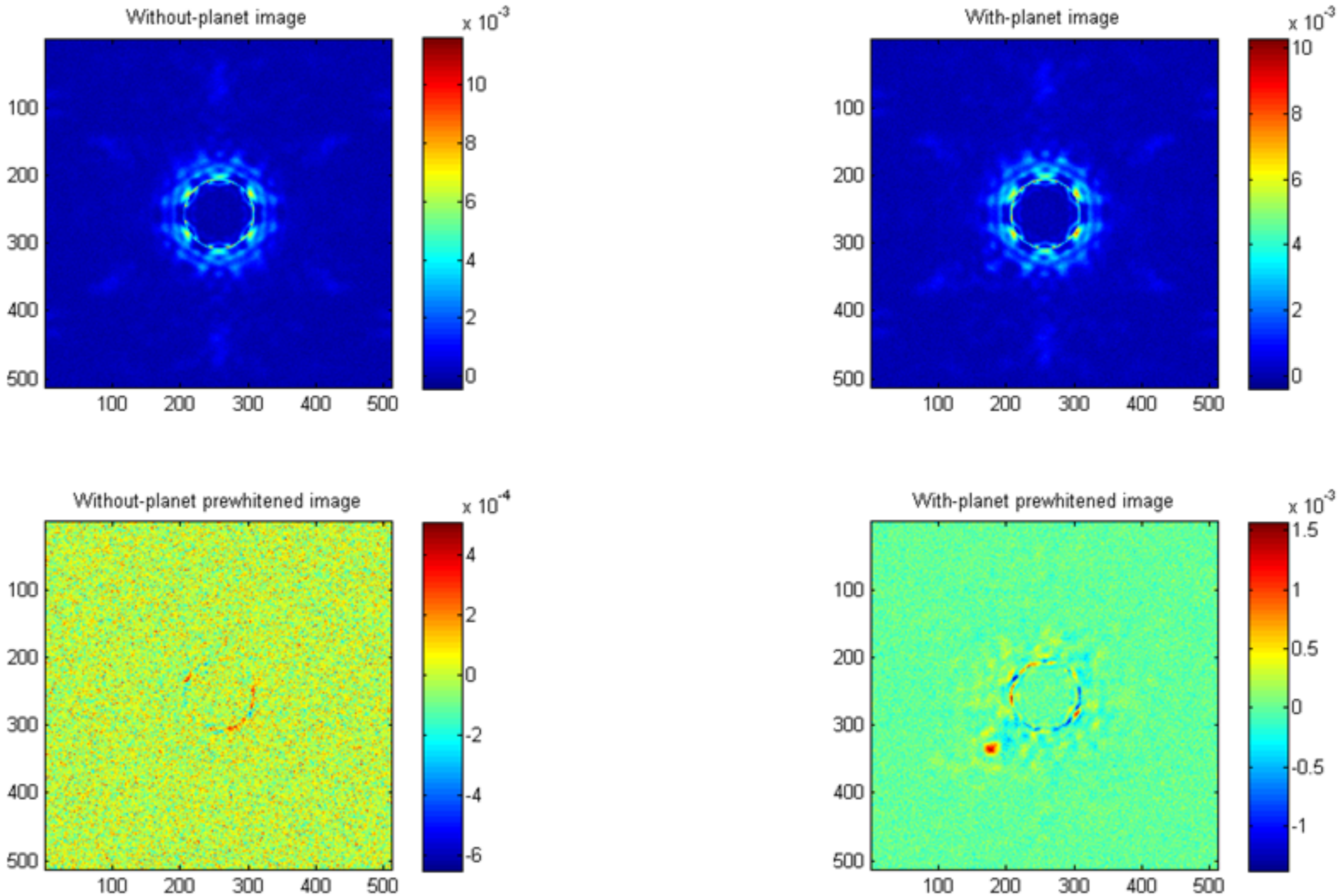

Coronagraph

Danielle Doughty
Kelsey Miller

Removing stellar light in order to resolve an Earth-size ETP with a ~1AU radius orbit around a Sun-type star at a distance of ~10ly whose PSF is ~10^{10} times dimmer than that of its parent star

Overview

- Possible candidate designs explored
- Why PIAACMC?
- What PIAACMC does/how it works
    - Resolution and throughput achieved with this coronagraph
    - Capabilities and Tradeoffs
- Theoretical Limits
- Placement of coronagraph in system
    - Why on each individual aperture and not after beam combining
    - Possible tradeoffs between putting coronagraph before vs. after beam combining

Coronagraph Candidates

- Conventional Pupil Apodization (CPA)
  - Not efficient at high contrast levels; poor angular resolution and high IWA

- Apodized Pupil Lyot Coronagraph (APLC)
  - Limited performance; trade-off between focal plane mask size and system throughput

- Apodized Pupil Complex Mask Lyot Coronagraph (APCMLC)
  - Apodization-related losses in throughput and angular resolutions are removed

- Phase-Induced Amplitude Apodization Coronagraph (PIAAC)
  - removes the throughput, angular resolution, and IWA losses introduced by the apodizer in above designs

- Phase-Induced Amplitude Apodization Lyot Coronagraph (PIAALC)
  - 1.8λ/D necessary for the desired 10^9 contrast

- PIAA Complex Mask Lyot Coronagraph (PIAACMC)
  - capable of 0.64 λ/D IWA at 10^{10} contrast with 50% throughput; at visible wavelengths and high contrast (above 10^8), the system does not show improvement over PIAA

Coronagraph Candidates

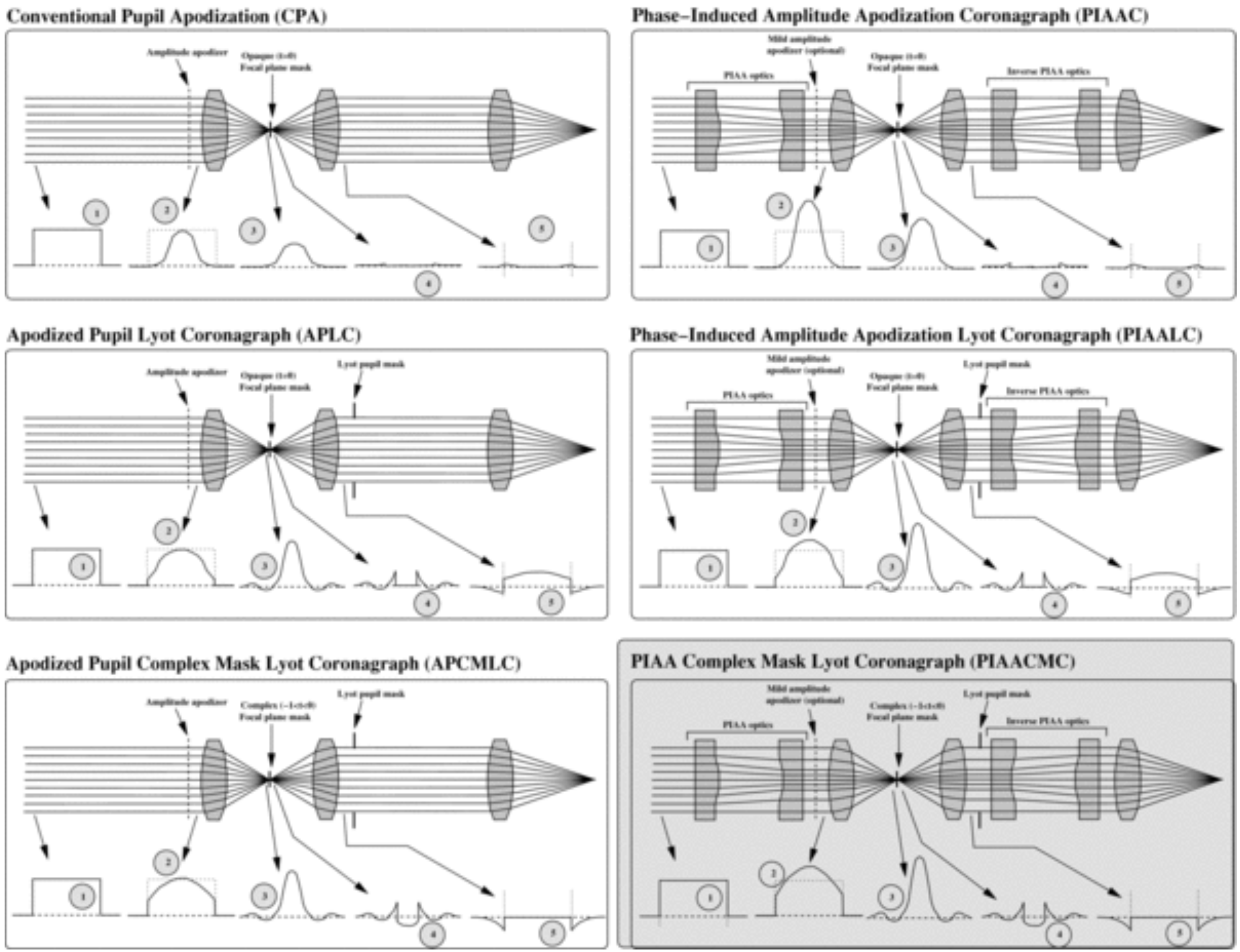

Coronagraph Candidates

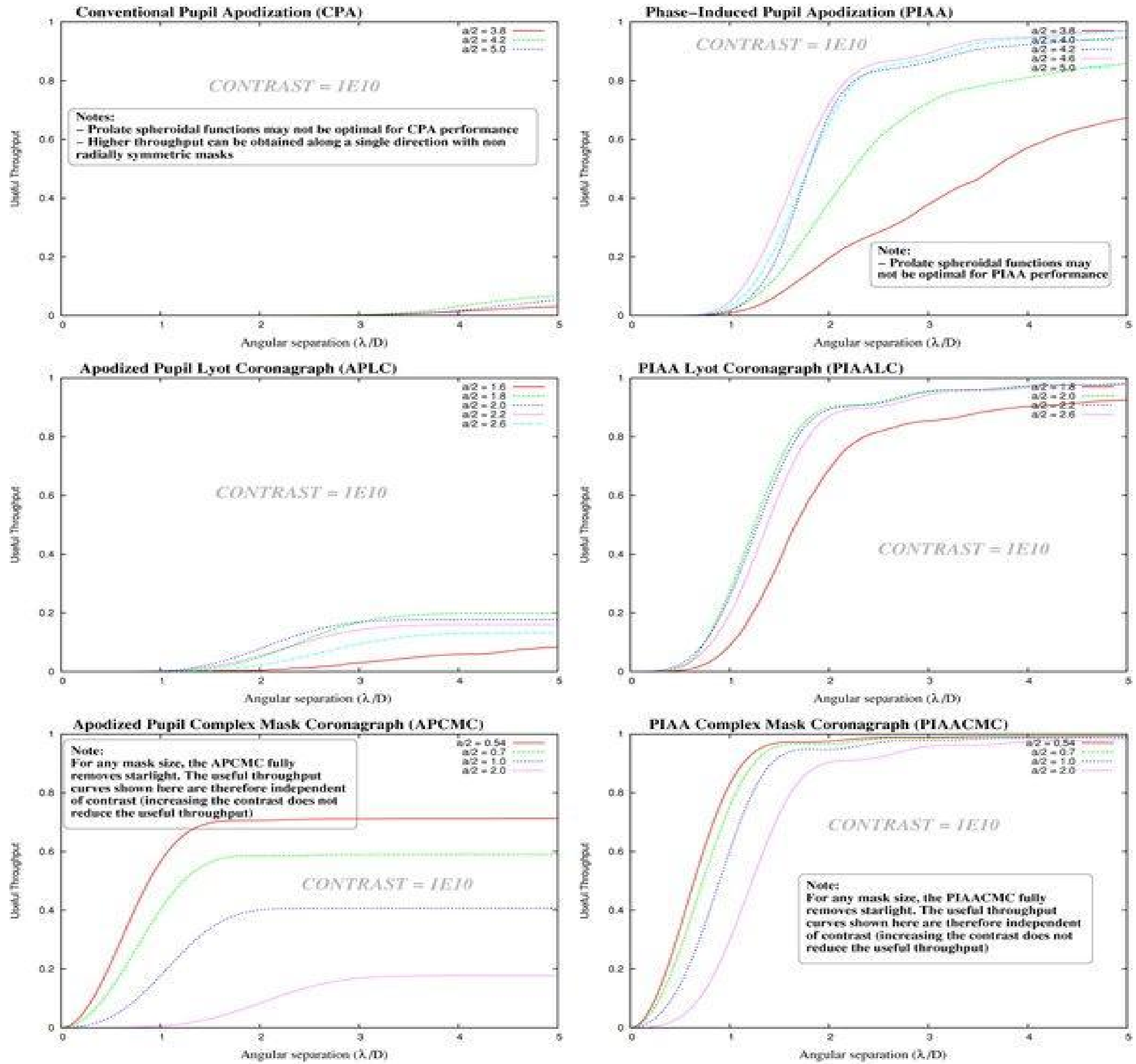

PIAACMC

Coronagraph that modifies the pupil by reflection on two mirrors with phase aberrations chosen to produce an exit pupil which greatly reduces the intensity of the PSF wings, allowing the light from the planet to be detected above the noise from the central star.

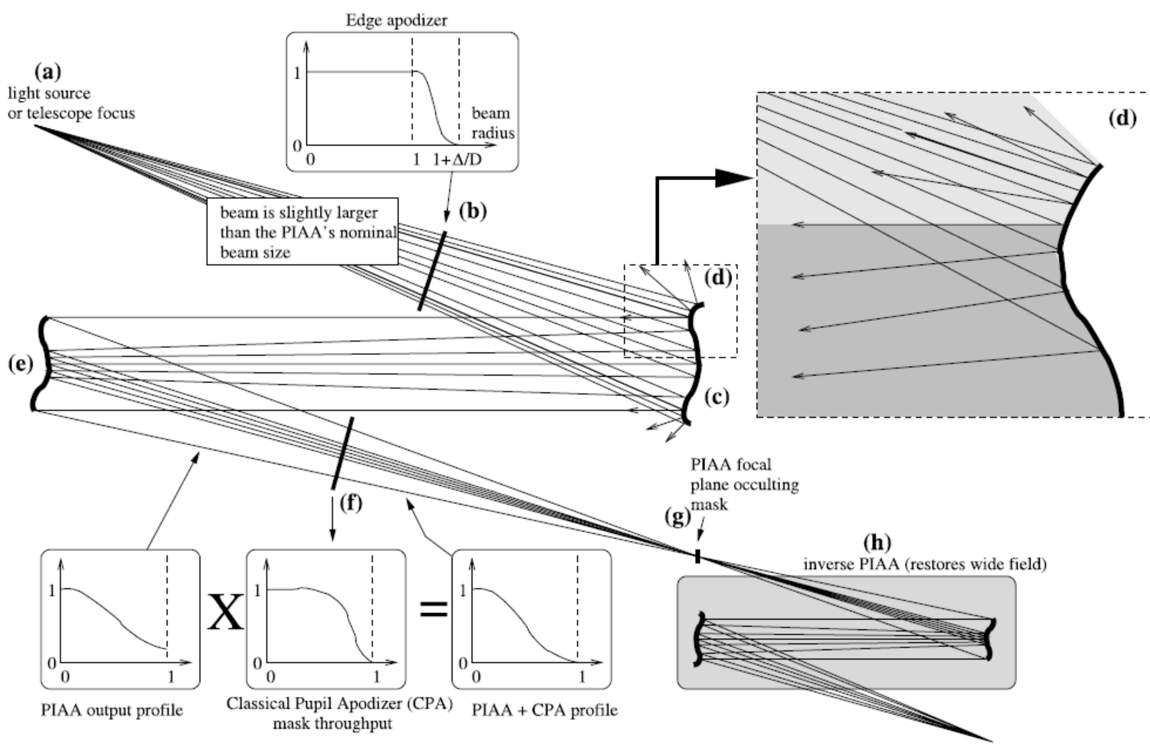

Inverse PIAA

The problem with the PIAACMC system is that it creates error in the off axis field of your image because you manipulated the input plane wave. This effect makes it so that your planet psf looks similar to coma aberration. To eliminate the effect we make use of an inverse PIAA system (which is the mirrors for the first portion reversed). Doing this cancels out our field aberrations we incurred and we are again dealing with a plane wave instead of a gaussian wave.

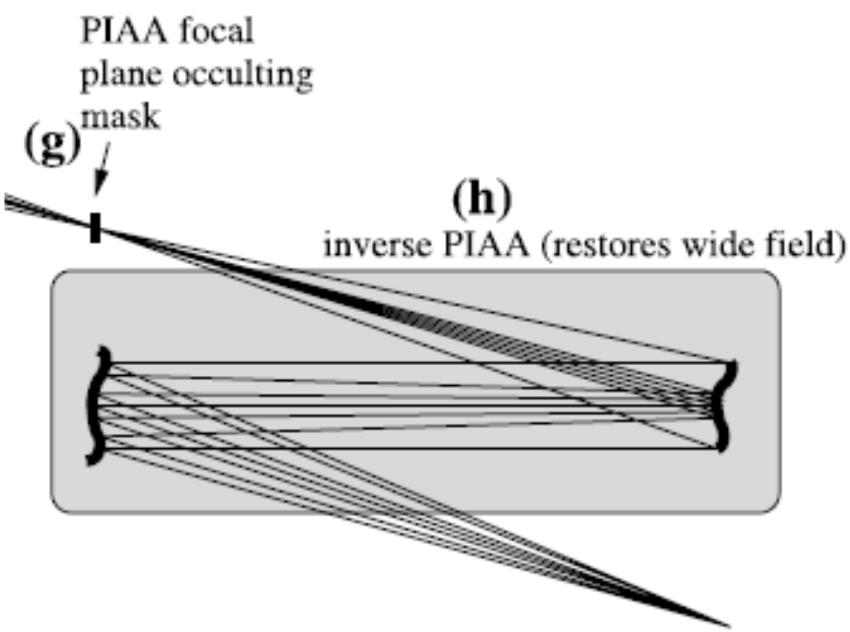

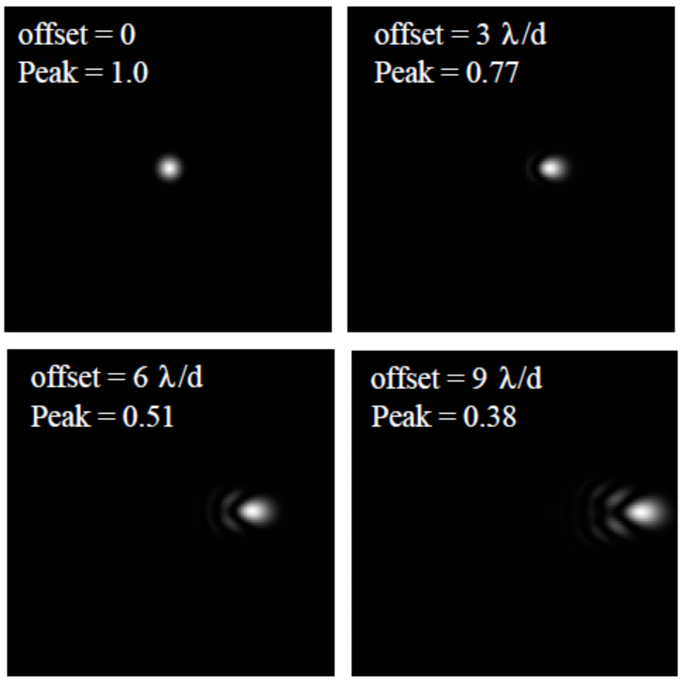

Fig. 5. Degradation of the PSF quality with distance to the optical axis for the example studied in Sect. 2.3. The brightness scale is linear and identical for all images.

Capabilities and Tradeoffs

The PIAACMC system is capable of:

- 0.64 lambda/D angular separation between the planet and the star but at the expense of 50% throughput
- ~1.2 lambda/D angular separation, ~96% throughput is possible

Repercussions:

With smaller IWA (i.e. 0.64 angular separation), the diameters of the individual apertures will increase due to:

$$n * \frac{\lambda}{D} = \frac{star\ - planet\ separation}{distance\ to\ star\ - planet\ system}$$

Where n is the defining coefficient (i.e. 0.64 or 1.2)

Because the total throughput will also go down (~50% for 0.64 lambda/D), aperture will have to increase even further to provide the necessary SNR for the science of the system

Theoretical Limit

Regardless of on-axis throughput a coronagraph with a circular pupil cannot have a usable throughput exceeding 50% at .5λ/D

This image shows the limit of detection ability of a companion (planet) being that as long as the flux of the companion is equal to the flux of the central source (parent star) then the planet should be resolvable.

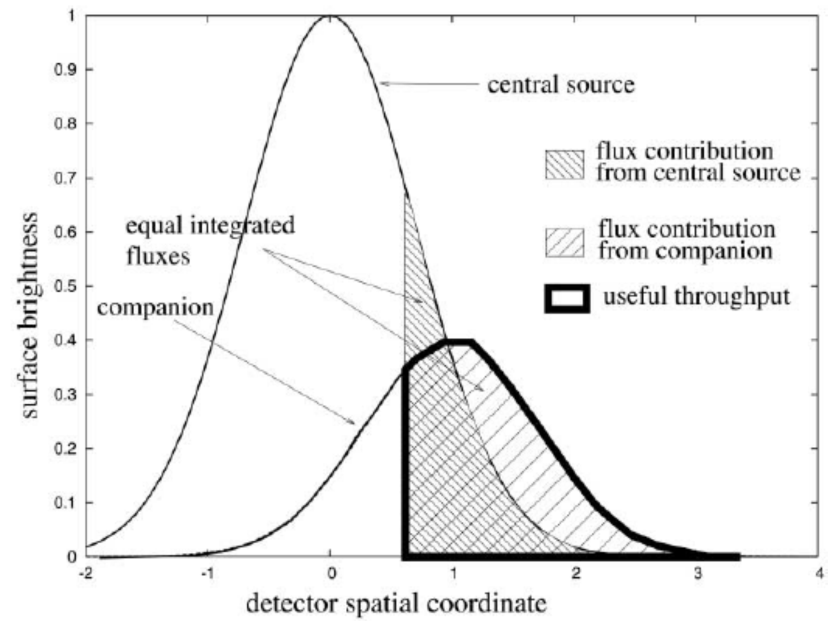

FIG. 2.—Graphical representation of the useful throughput. In this one-dimensional example, the stellar and planet PSF are shown with some overlapping. The useful throughput is obtained by integrating the companion (planet) light from $x \approx 0.7$ to $x \approx 3.2$; in this interval, the integrated flux contributions from the central source and the companion are equal.

Placement in System

Configuration Options

- After beam combination
  - Pros:
    - smaller λ/D (IWA); D = B (baseline of array)
  - Cons:
    - edge effects and aberrations from individual apertures compounded and difficult to remove
- Before beam combination
  - Pros:
    - easily fix edge effects with apodized entrance pupil (low pass filter)
    - only interfering planet light
    - Simpler design (for one aperture input rather than multiple)
  - Cons
    - Larger λ/D (IWA); D = (individual aperture diameter)

Coronagraph sensitivity to stellar size:

With the PIAA system we are less sensitive to stellar size than other coronagraphs. But, there is still an effect that we need to take note. Our useful throughput will decrease as the stellar radius increases due to a higher number of lobes present that need to be removed. This causes the coronagraphs blind spot to increase by a factor of (lambda/d)^2 in the focal plane. Meaning that increasing our stellar radius to a factor of .1lambda/d causing the 50% theoretical limit to shift our IWA to almost 2lambda/d from .5lambda/d. Thus, with an increase in stellar diameter our ability to look at planets close to the host star decreases.

Since our planet is brighter in the IR than in the visible we are able to get away with 10^6 -10^7contrast rather than 10^10 if we were to work in the visible, thus why we are working at 10um.

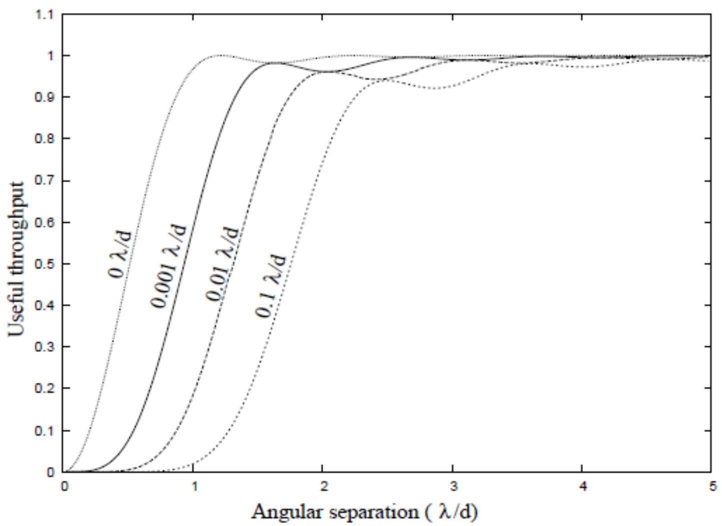

Fig. 9.— Upper limit on the off-axis throughput of a coronagraph for different stellar radii.

Optical / Mechanical Design

Alex Felli
Alex Rodack
Nick Thelin
Nate Wilkerson

Design Constraints-Array

- How many telescopes? (16)
- # of Baseline? (120)
- Array Shape? (parabolic)
- FOV? (arcmin or arcsec order)
- Sag Calculations: $R^2 = 4*D*F$
- Positioning (free-flying) and Rotation capability

2D Schematic of Parabolic 2D

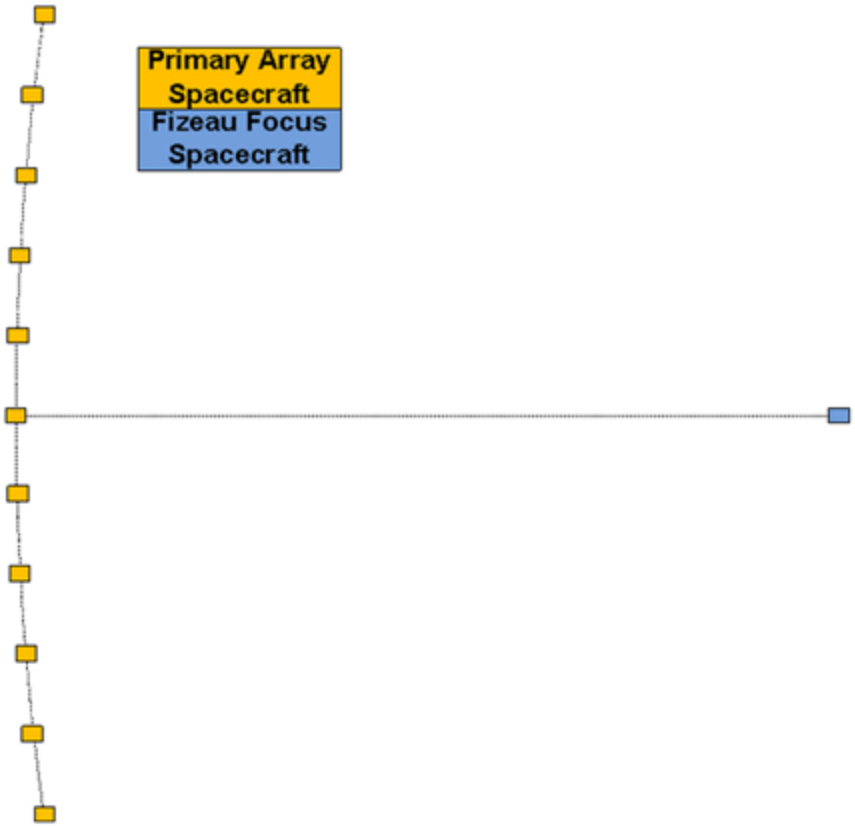

- Radius of Array: 189 km
- f/1 system:
- Focal length = 390 km (location of Fizeau Focus)
- 16 Individual Apertures, located in a non-redundant system

Design Constraints-Apertures

- Afocal Primary (Mersenne)
- FOV (order of degrees for tracking)
- Diameter of 4.5m
- Consideration of off-axis parabolic wavefront out to Fizeau (different for all apertures)
- Location of AO and Coronagraph sub-systems

Actual Sub-Aperture Layout

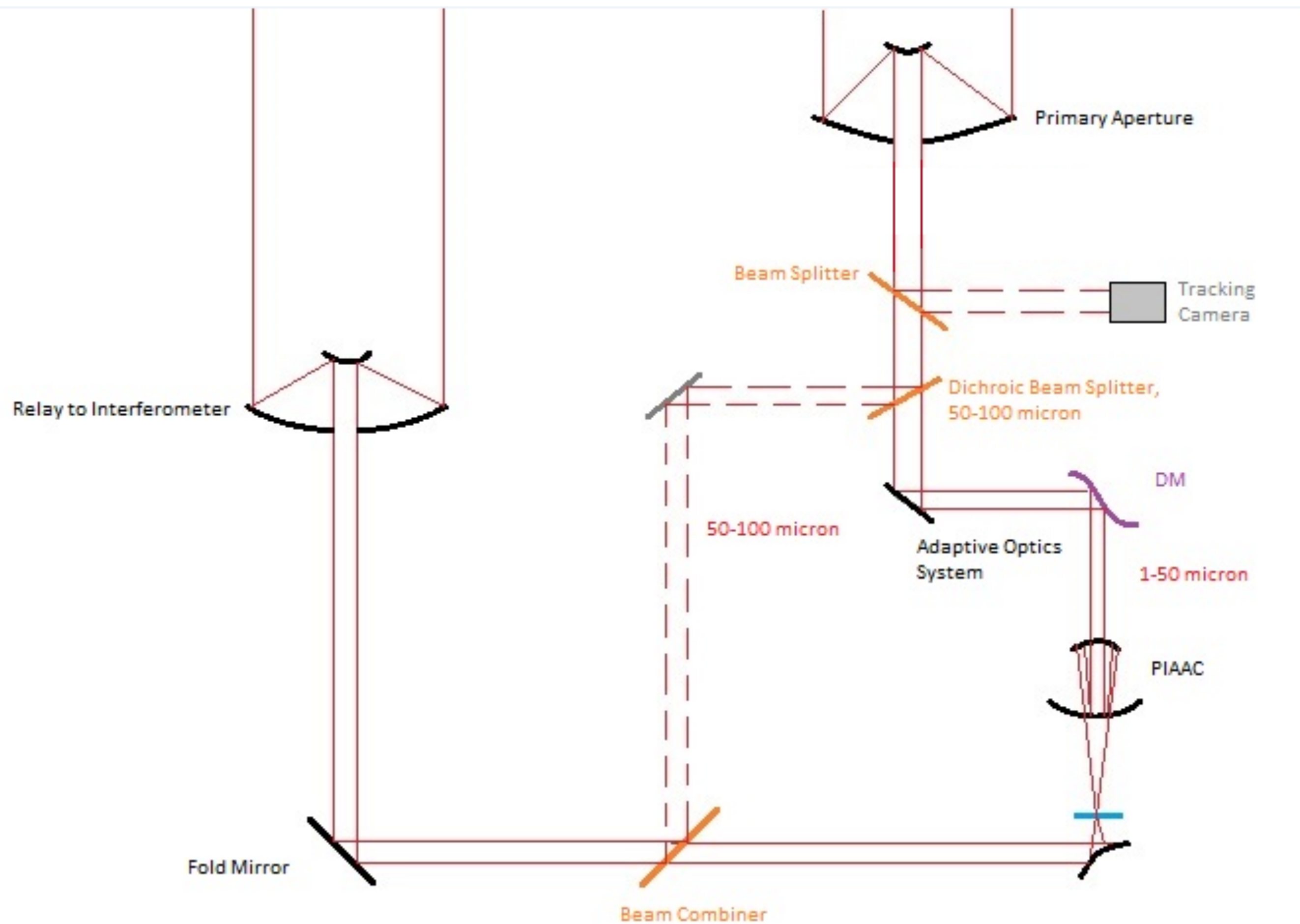

Sub-Aperture Telescope Design

- 2 Afocal Mersenne telescopes/sub-aperture
- Concave parabolic primary mirror
- Convex parabolic primary mirror
- Forms image at infinity to relay collimated light through the system

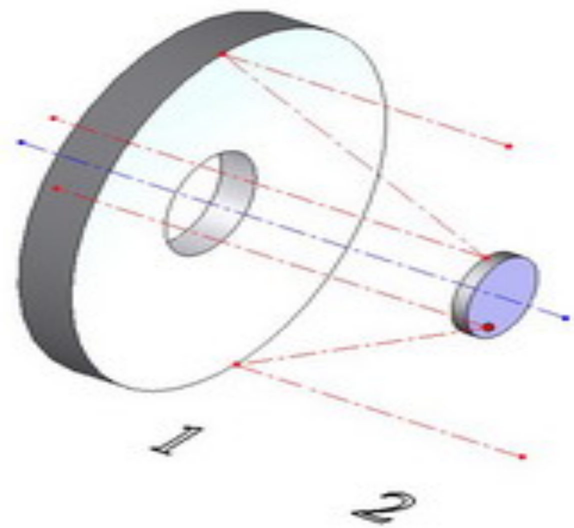

2D CodeV Sketch of Sub-System

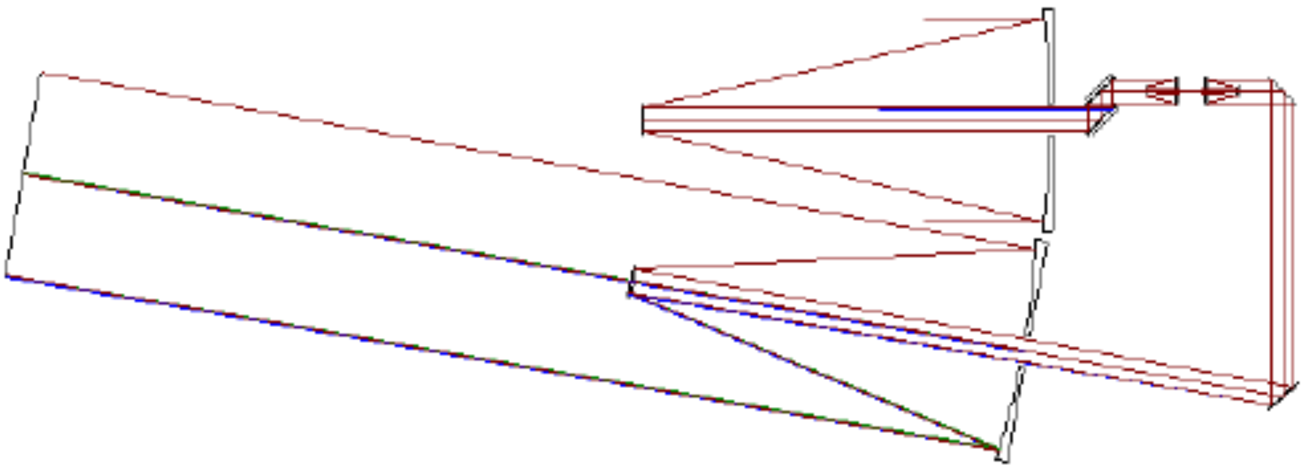

CodeV Design of Sub-Aperture System

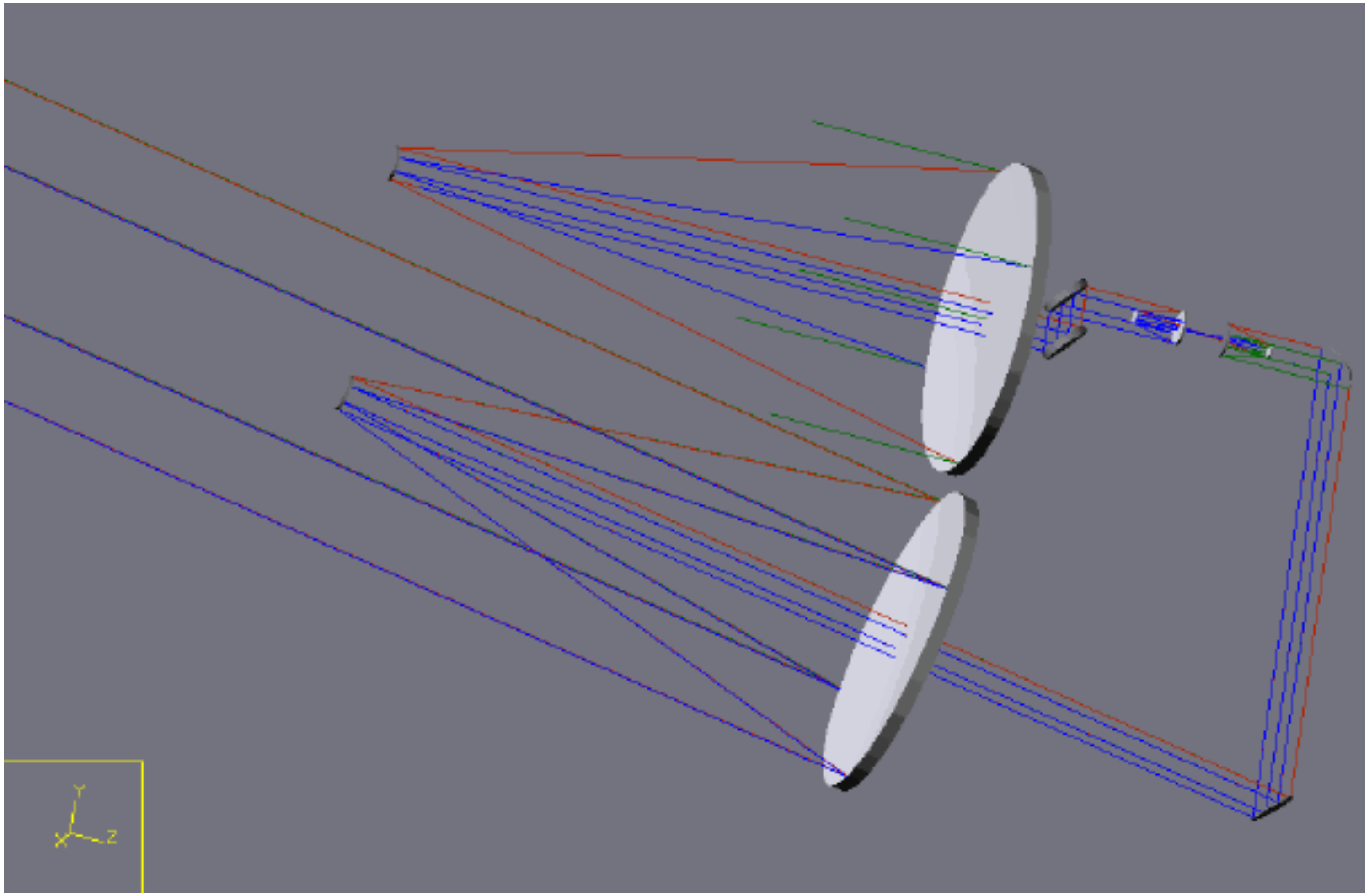

CodeV Design Zoomed In

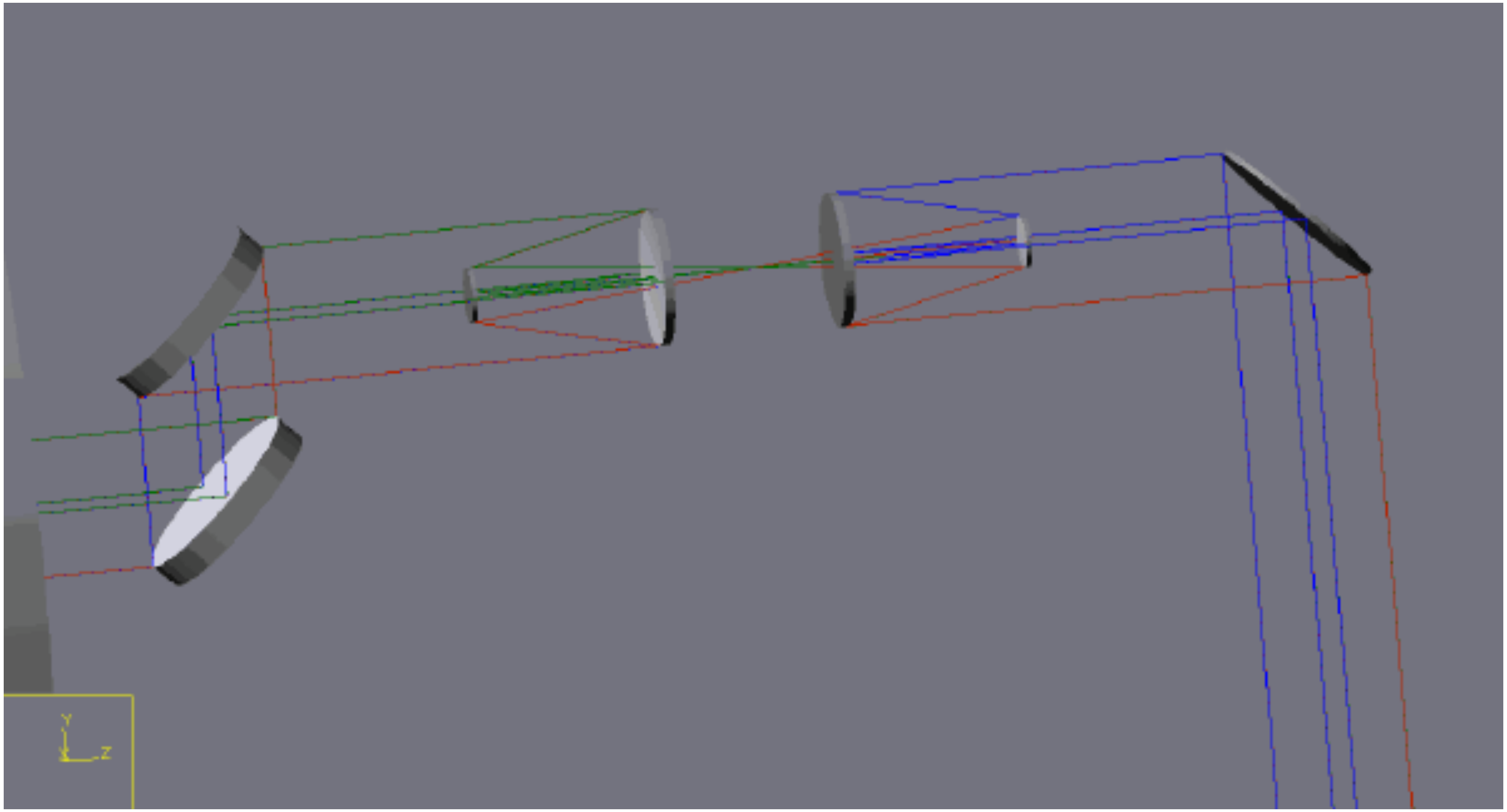

Mechanical System

To Scale View of System

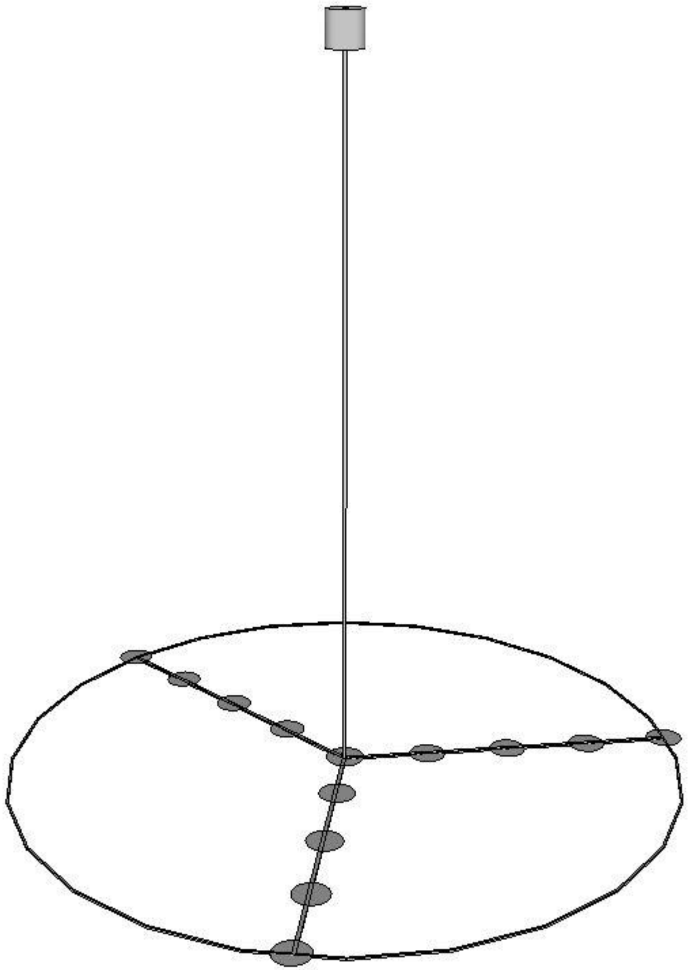

Receiving & Transmitting Apertures (Cassegrain)

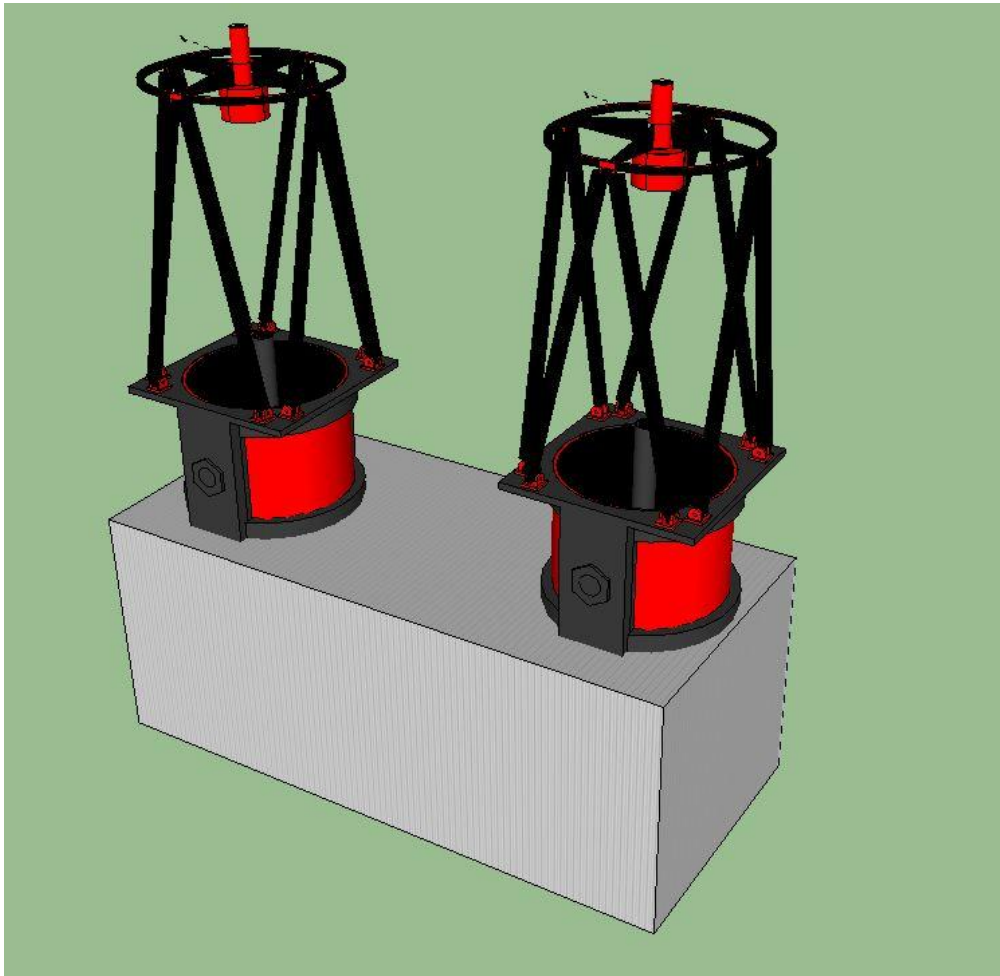

Re-imaging System at Front of Structure

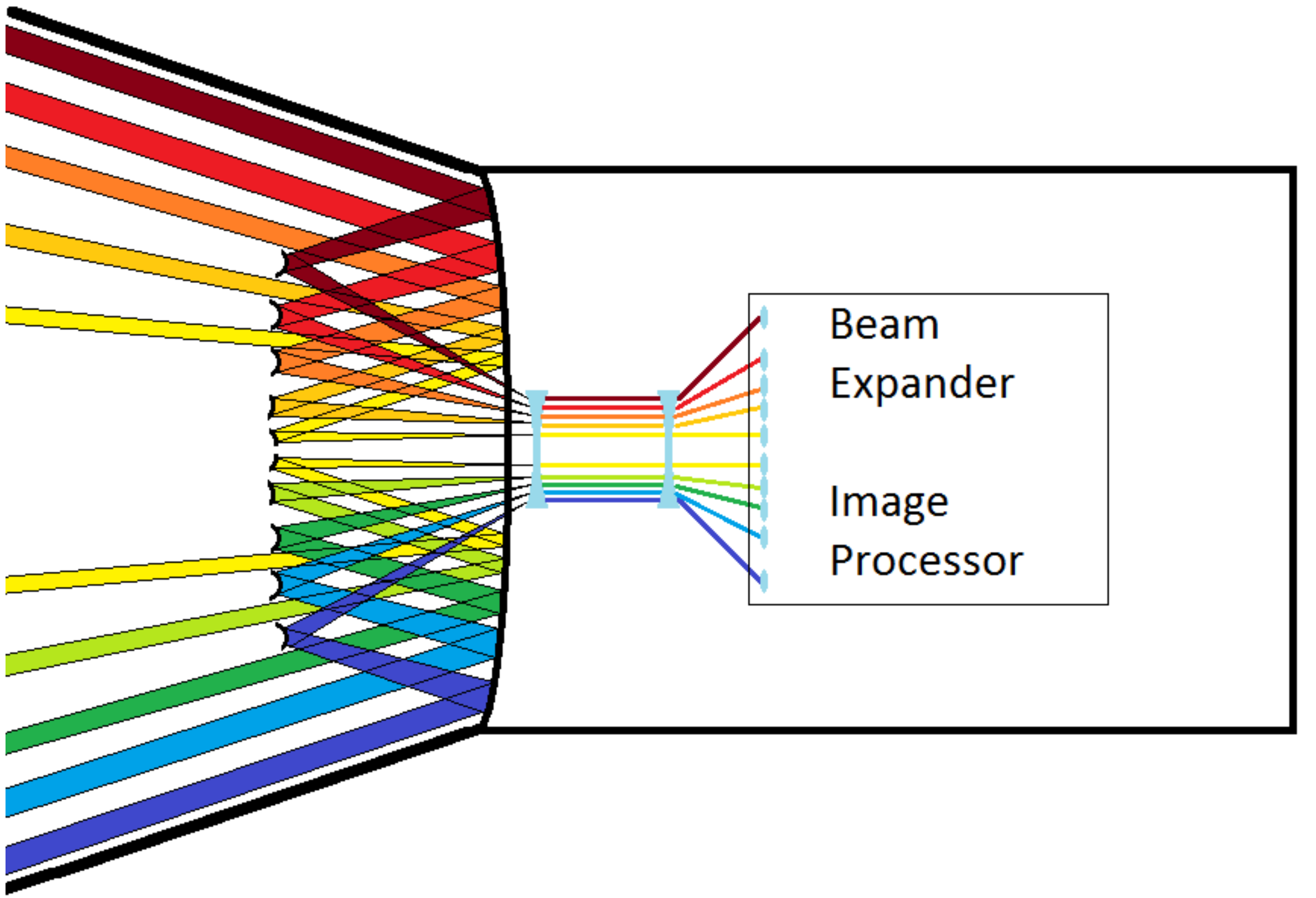

Interferometry

Soha Namnabat
Xiaoyin Zhu

Interferometry Overview

Main Beam Combiner

Pupil Densification

Detector (What kind? Size?)

Beam Combiner

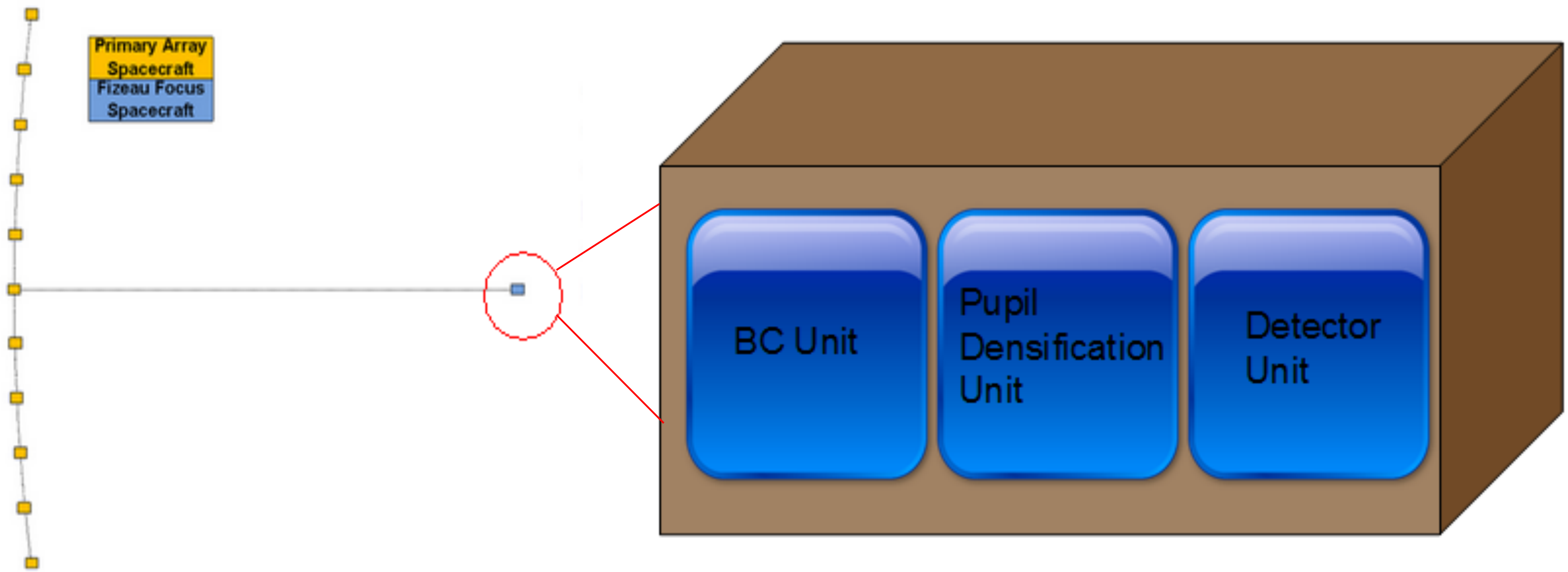

The Beam Combiner is the heart of the interferometer. The starlight beams from each arm are directed to the beam combiner where they are interfered. Therefore, the BC contains all of the optics and detectors for measuring fringe characteristics.

Beam Combiner

Two types:

1. Combine the beams at an angle, forming interference fringes across the image as in Young's double slit experiment;

2. Combine the beams in parallel and form fringes by changing the optical path of one arm with respect to the other.

Beam Combiner

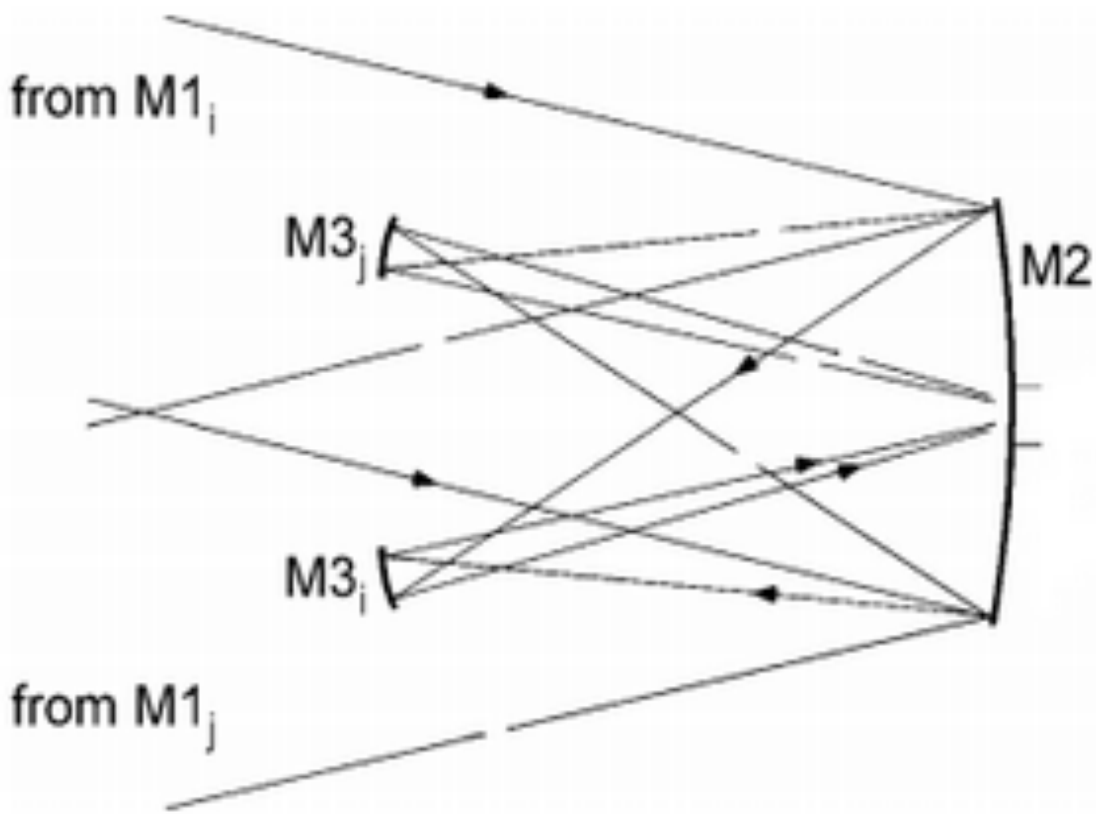

To capture most of the light diffracted from a subaperture of size d into a beam-combiner located at distance L requires a collecting aperture of size d larger than the Airy peak. The condition can be written $\lambda L/d < d'$.

Pupil Densification

Densification is a key system for these hyper telescopes. It is what makes a hypertelescope acts as a regular telescope.
Pupil densification increases the pupil filling factor by bringing the sub-pupils closer to each other,therefore artificially increasing D=B and reducing the number of diffraction peaks in the PSF. It “magnifies” the diffraction pattern inside the envelope.
When the pupil is fully densified, only one bright diffraction peak is inside the PSF's envelope.

Pupil densification of a sparse array of apertures creates a PSF close to a single-aperture telescope's PSF

A&A 391, 379–395 (2002)

Pupil Densification

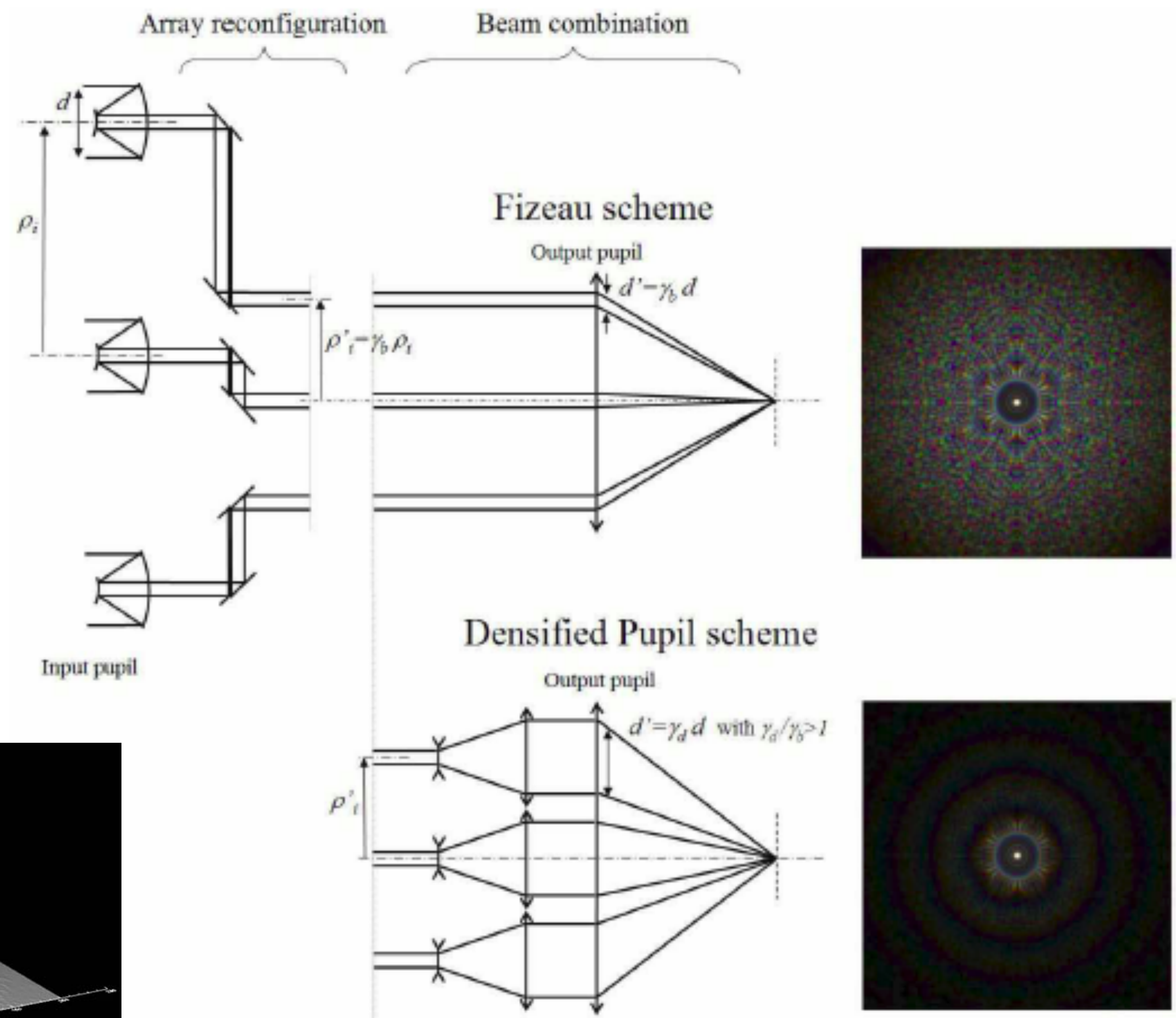

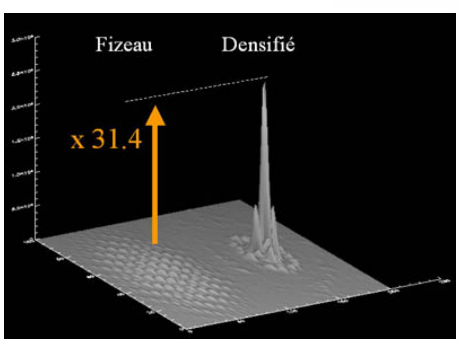

Mon. Not. R. Astron. Soc. 000, 1–?? (2006)

Pupil Densification

Fizeau image through an interferometer of base B, pupils diameter d.

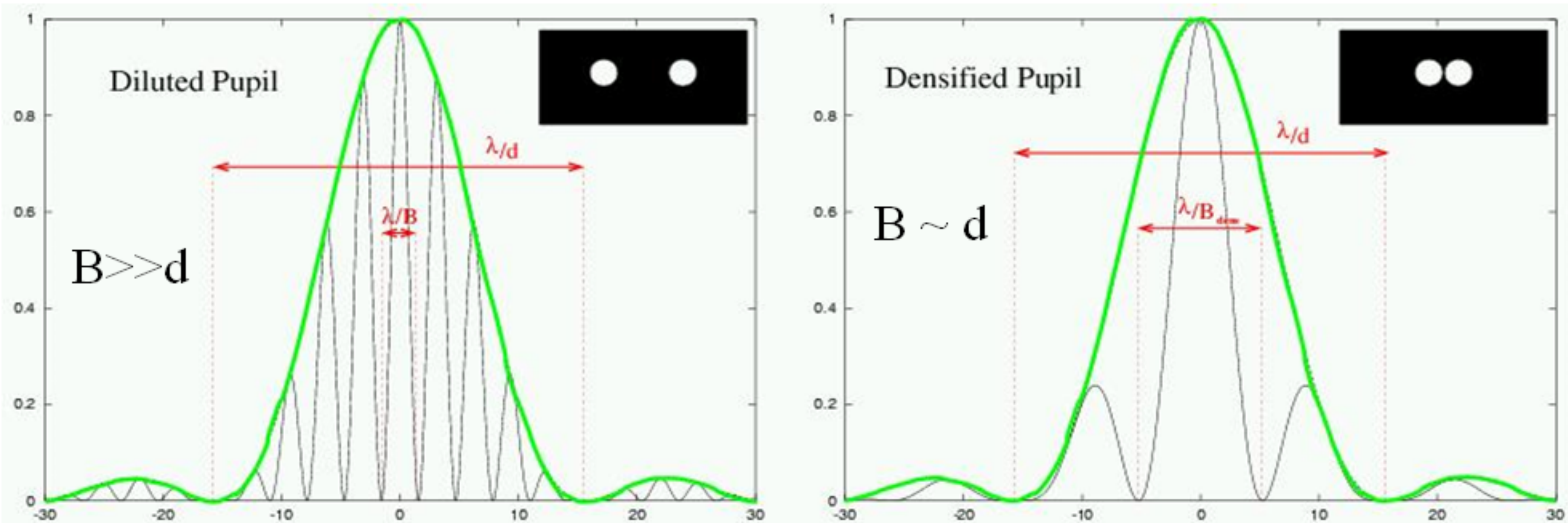

Good angular resolution
Many diffraction peaks
-> little light per peak
-> need big detector
-> not compatible with coronagraphs

1 single peak
-> contrasted PSF
-> small detector OK
-> compatible with coronagraphy
poor angular resolution

Pupil Densification (Labeyrie, 1996) Array geometry is preserved

PSF is invariant by translation within a small field of view (Zero Order Field, ZOF).

-> ***Hypertelescope***

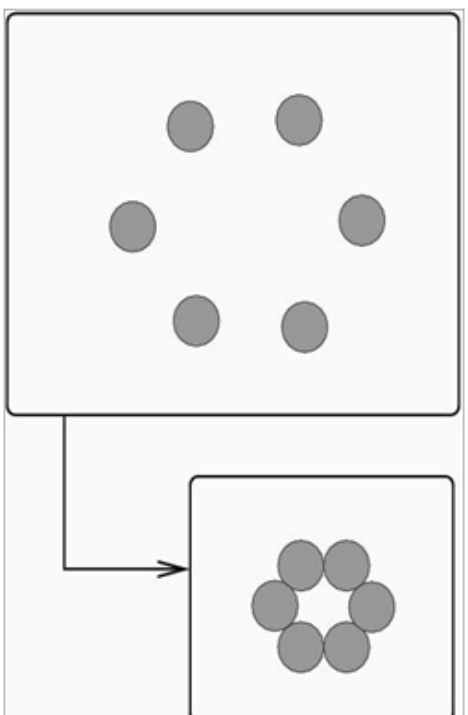

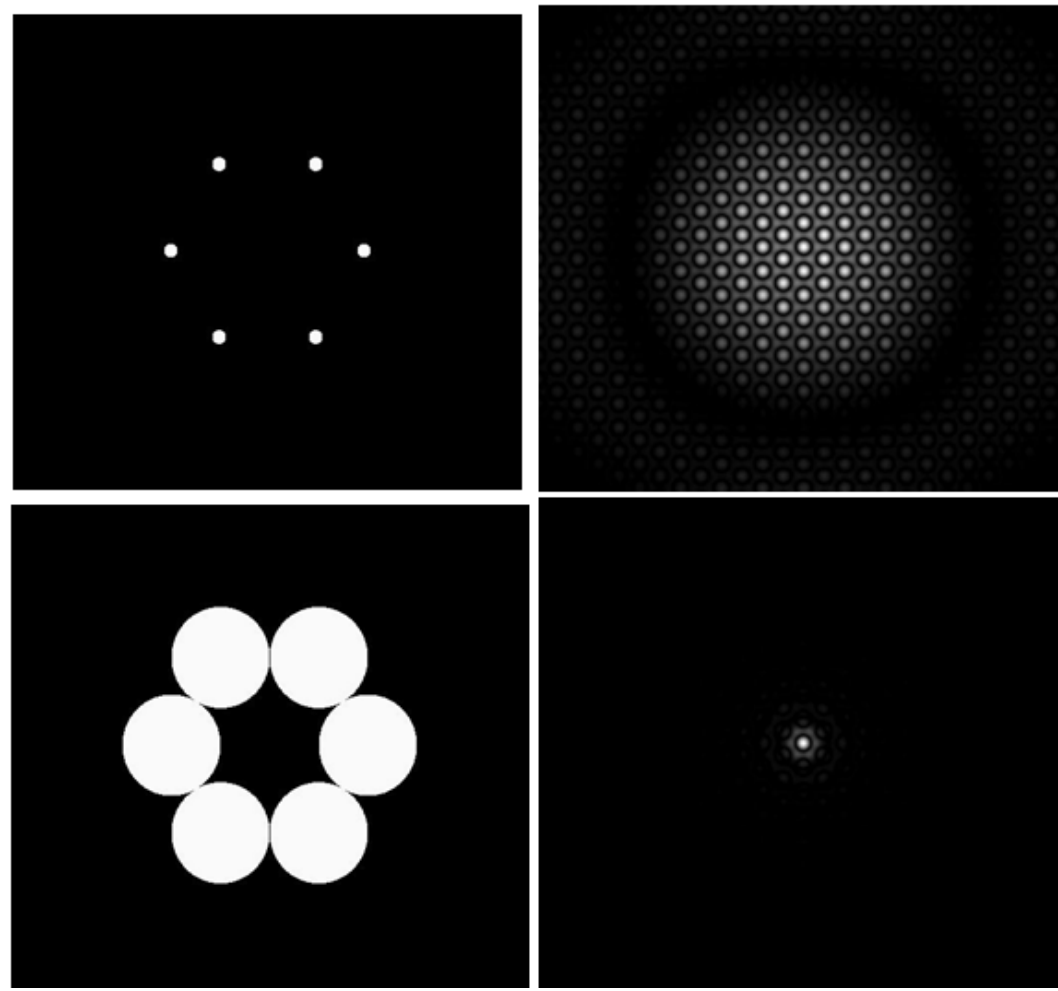

Pupil densification - FOV comparison

Densification limits the FOV in our image plane such that planet is not observed. So to observe the planet, we must tip tilt the densifier elements to locate the envelope on the planets fringes.

Table 2. Field of view and number of diffraction peaks of the PSF in the densified pupil and diluted pupil schemes. N is the number of apertures, B the baseline and d the diameter of individual apertures.

	Densified Pupil	Diluted Pupil
Field of View	Useful FOV $\sqrt{N} \times \frac{\lambda}{B}$	No limitation
Number of diffraction peaks	1	$\left(\frac{B}{d\sqrt{N}}\right)^2$

Pupil Densification

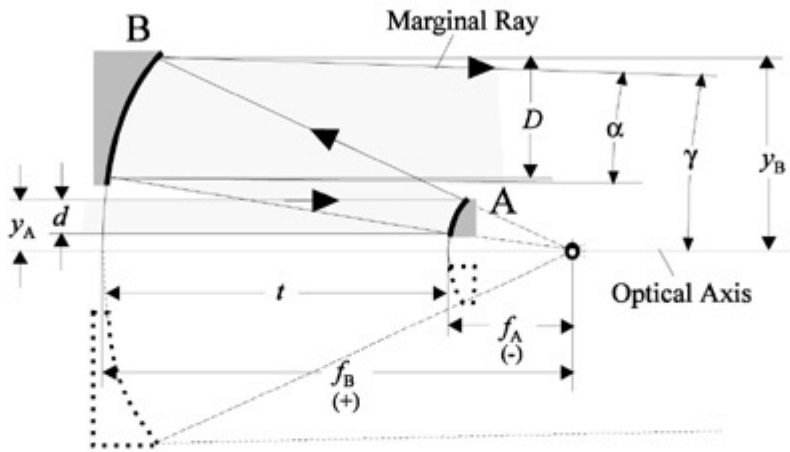

Figure 1 *Cassegrain beam expander.*

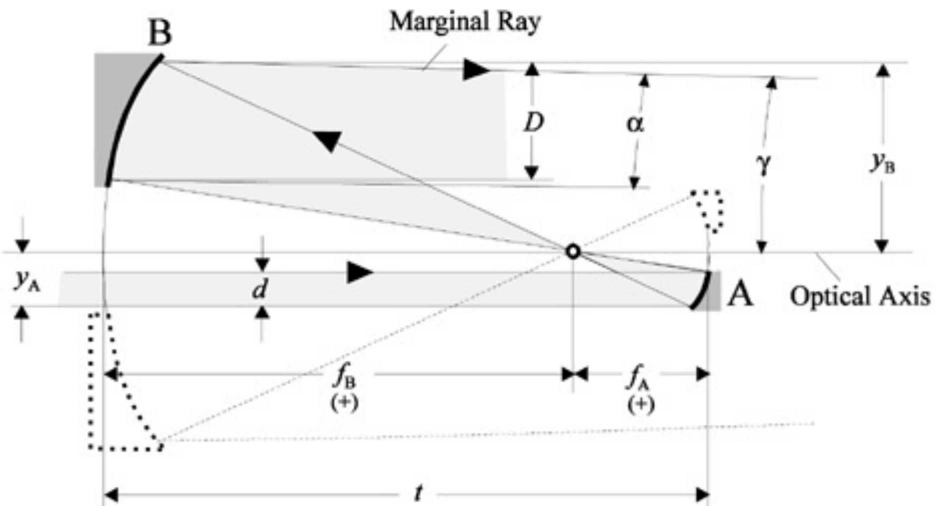

Figure 2 *Gregorian beam expander.*

Beam Expander is needed for densification of the pupils.

Two reflective beam expanders exist : Cassegrain and Gregorian

The mirrors should be asphere to avoid spherical abberation

http://spie.org/x34466.xml

Pupil Densification - Imaging

Final imaging would be done with a cassegrain which is large enough to cover all the cassegrain beam expanders.

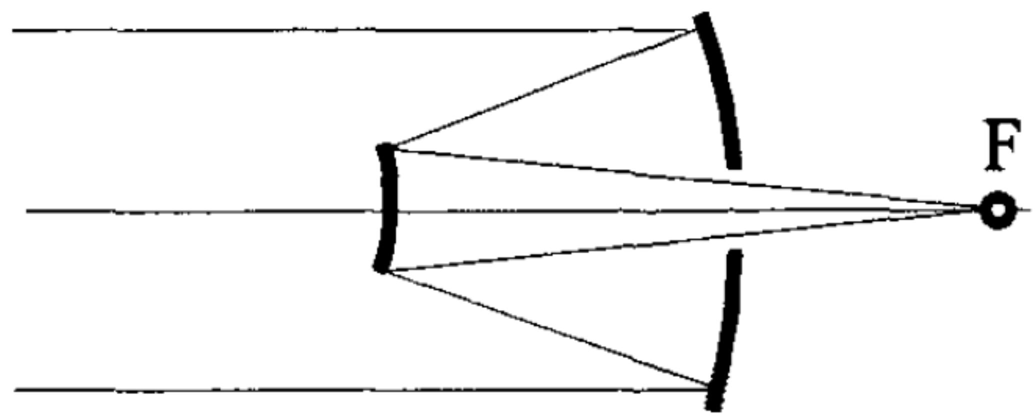

Cassegrain

Detector specs

optically smallest spatial feature resolvable : λ/B
(optical pixel)

Nyquist Sampling says sampling frequency is twice the bandwidth of signal

so each optical pixel = 2 detector pixel minimum

detector pixel = $\lambda/(2B)$ @ 1 um (smallest wavelength for detection)

End